Environmental Science Nano

ROYAL SOCIETY OF CHEMISTRY

CRITICAL REVIEW

Check for updates

Cite this: *Environ. Sci.: Nano*, 2021, **8**, 1835

Porous graphitic carbon nitride nanomaterials for water treatment

Xiuqin Huo,†[ab] Huan Yi,†[ab] Yukui Fu,[ab] Ziwen An,[ab] Lei Qin,[ab] Xigui Liu,[ab] Bisheng Li,[ab] Shiyu Liu,[ab] Ling Li,[ab] Mingming Zhang,[ab] Fuhang Xu,[ab] Guangming Zeng *[ab] and Cui Lai *[ab]

Received 20th February 2021,
Accepted 17th May 2021

DOI: 10.1039/d1en00171j

rsc.li/es-nano

The search for suitable functional materials is indispensable to solve the increasing worldwide wastewater pollution. Accordingly, porous graphitic carbon nitride (PCN) with an adjustable electronic/atomic structure has been a hot topic owing to its desirable properties of large surface area, excellent stability, strong electron transport ability, low cytotoxicity, and antibacterial and antiviral activity. Previous reviews mainly focused on the application of PCN in photocatalysis; however, its application in adsorption, reduction and other AOPs for water treatment is rarely reported, especially for actual water treatment. This review firstly summarizes the modification of PCN including morphology control, defect engineering, doping engineering, hybridizing strategy and anchoring single atoms, which can adjust the electronic structure and enhance its catalytic properties. Then, we systematically summarize functional modified porous graphitic carbon nitride (FPCN) used in adsorption, reduction, and AOPs for water treatment including the degradation of organics, landfill leachate control, constructing membrane systems, water disinfection and microbial control, with emphasis on actual water treatment that is closely related to daily life. Finally, the existing challenges and development prospects of PCN are proposed from theoretical calculation to its practical application. This review provides an in-depth understanding of PCN and presents insight into its application in different technologies for actual water treatment, and we believe that this review will be beneficial for further research.

Environmental significance

Nanomaterials have been widely used for solving the increasing worldwide wastewater pollution. Thus, the porous graphitic carbon nitride (PCN) nanomaterial with the properties of large surface area, strong electron transport ability, low cytotoxicity, and antibacterial and antiviral activity has attracted great attention. To the best of our knowledge, previous reviews mainly focused on the application in photocatalysis over PCN, and its application in adsorption, reduction and other AOPs for water treatment especially actual water treatment is lacking. In this review, we firstly summarize the functional modification of PCN, which is conductive to enhance its catalytic property for the removal of pollutants in wastewater. Then, we systematically summarize PCN used in adsorption, reduction, and AOPs for water treatment. Most importantly, PCN applied in water disinfection and microbial control is discussed, which is closely related to the safety of our drinking water. Finally, the existing challenges and development prospect of PCN are proposed, ranging from theoretical calculation to its practical application.

1. Introduction

The energy crisis and environmental issues have become serious threats to sustainable economic development.[1] Notably, water contamination caused by organics with complexity and inflexibility, such as dyes, phenols, pharmaceuticals, and personal care products, has become a serious problem.[2–5] Accordingly, adsorption, reduction, and advanced oxidation technologies (AOPs) have been considered efficient technologies to address these issues. Adsorption is simple technology to eliminate contaminations on a large scale.[6–8] The reduction process can transform highly toxic organic pollutants into low toxic ones with strong operability and high efficiency.[9] Common AOPs, such as photocatalysis,[10,11] photoelectrocatalysis (PEC),[12] Fenton and Fenton-like oxidative technology,[13–15] are used for the degradation of these contaminants.[16] This is because highly reactive species (RS) are generated to participate in AOPs, which show enhanced redox performances for

[a] *College of Environmental Science and Engineering, Hunan University, Changsha, Hunan 410082, China. E-mail: zgming@hnu.edu.cn, laicui@hnu.edu.cn; Fax: +86 731 88823701; Tel: +86 731 88822754*
[b] *Key Laboratory of Environmental Biology and Pollution Control (Hunan University), Ministry of Education, Changsha, Hunan 410082, China*
† These authors contribute equally to this article.

contaminations. Based on the above analysis, it is crucial to search for suitable catalysts for these processes.

Graphitized carbon nitride (g-C_3N_4), a non-metal and non-toxic polymer semiconductor synthesized *via* simple thermal condensation with nitrogen-rich precursors,[17] has been widely used in catalysis for the degradation of contaminants.[18] However, the resulting bulk g-C_3N_4 (BCN) always exhibits unsatisfactory catalytic efficiency due to the rapid recombination of charge carriers, its small surface area, and low visible light utilization efficiency.[19,20] Therefore, it is imperative to modify g-C_3N_4 to enhance its catalytic performance. Porous carbon nitride (PCN) with an adjusted morphology/porosity and electronic/atomic structure has gradually gained widespread attention. Cross-plane electron diffusion channels are provided by its porous structure, and the number of recombination sites of photogenerated electrons is also reduced. Besides, the porous structure can suppress the interlayer stacking due to the reduced number of interaction sites.[21] Furthermore, other features, such as the high physicochemical stability and particular supported properties of PCN make it a potential metal-free polymeric semiconductor for application in wastewater treatment.[22,23] For example, PCN has been widely used in the adsorption and degradation of organics,[7] dyes[24] and heavy metal ions.[25] Microorganisms such as bacteria and algae are also eliminated by PCN owing to its low cytotoxicity,[26] and antibacterial[27] and antiviral[28] activity.

In the literature, there are a few relevant reviews summarizing the preparation, modification and application of PCN.[29,30] However, focus on its the application in wastewater treatment is absent, especially for actual water treatment. Therefore, this review emphasizes the application of PCN for wastewater treatment. On account of the limitations of PCN, it is essential to give a brief description of its modification. Many functional modifications of PCN, including morphology control, defect engineering, doping engineering, hybridizing strategy and anchoring single atoms, have been employed to provide more active sites, enhance its absorption capacity and suppress electron–hole recombination. These functional modified strategies can further tailor the unique properties of PCN for optimizing its potential applications.[31] Therefore, we discuss the application of these functional PCN (FPCN) in water treatment, including the removal of organics, leachate control, constructing membrane systems, water disinfection and microbial control. Finally, the existing challenges and development prospects of PCN catalysts are presented, which is anticipated to provide significant guidance for water treatment (Fig. 1).

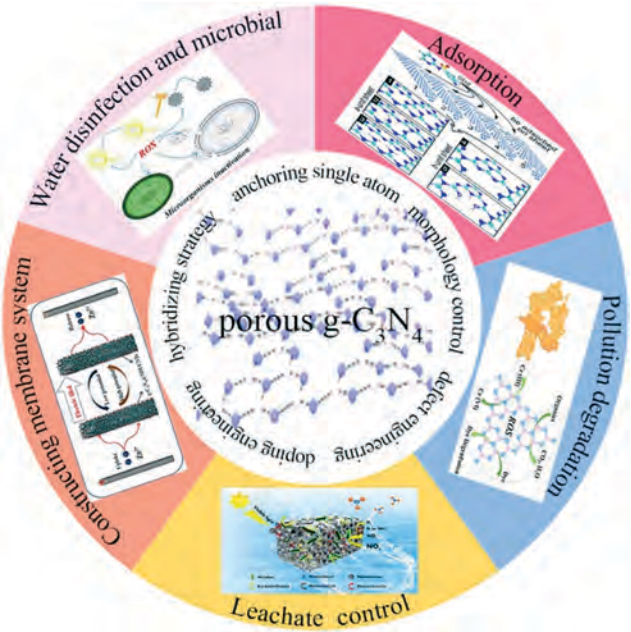

Fig. 1 Illustration of the modification and applications of porous g-C_3N_4 nanomaterials for water treatment.

2. Functional modifications

There are two ways to synthesize PCN. The first involves the use of nitrogen-rich precursors to directly fabricate PCN with a template or intermolecular force, which is a bottom-up method. This method can avoid the destruction of the planar atomic structure and is mainly used at present. The second is the chemical exfoliation or thermal oxidization of bulk g-C_3N_4, which is a top-down method. The typical synthetic methods and properties of PCN are listed in Table 1, and thus no further details are discussed. However, the poor visible light utilization and ultrafast carrier recombination of PCN still limit its application. Therefore, in this section, we mainly focus on the functional modification of PCN, including morphology control, defect engineering, doping engineering, hybridizing strategy and anchoring single atoms, to solve these problems and enhance its catalytic activity.

2.1 Morphology control

Generally, nanostructured g-C_3N_4 semiconductors with unique morphologies attract significant attention on account of their specific surface area. For instance, macro-/meso-porous g-C_3N_4 with nanosheet, nanofiber, and nanosphere structures have been explored to meet practical applications. In numerous reports, ultrathin nanosheet structures exhibit superior photocatalytic performances, especially shorter charge migration distances.[42] Therefore, many efforts have been explored to synthesize two-dimensional (2D) ultrathin g-C_3N_4 nanosheets.[43,44] The interlaminar van der Waals force of g-C_3N_4 is weak, and therefore it is possible to synthesize ultrathin g-C_3N_4 nanosheets *via* chemical exfoliation. Different etchants, such as strong acids,[45,46] isopropyl alcohol,[47] and other highly oxidizing materials,[48] can change the morphology and porosity of PCN due to different reaction mechanisms. In the treatment of $K_2Cr_2O_7$–H_2SO_4, hydroxyl and carboxyl groups were produced through acid oxidation. The hydrophilic functional groups were inserted in the

Table 1 Summary of the synthetic strategies for PCN

Synthesis strategy	Synthetic method	Template/etchant	Precursor	Morphology	Sample	Application	Ref.
Bottom-up approaches	Hard template methods	Mesoporous silica	Urea and dicyandiamide	Nano-layer with irregular holes	Mesoporous CuO/g-C_3N_4	Hg(II) photoreduction	32
		KIT-6	Cyanamide	Ordered mesoporous nanocasted	m-CN	RhB degradation	33
		Crab shells	Urea	Porous nanofibers	g-C_3N_4–T	U(VI) elimination	34
		Calcium carbonate	Melamine	Nanoporous sheets	npg-C_3N_4	MB adsorption and degradation	35
	Soft template methods	NH_4Cl bubbles	Ammonium chloride and melamine	Nanoporous sheets	CN–Cl	TC degradation	36
		CTAB	Melamine	Porous nanosheets	mpg-C_3N_4	MB degradation	37
	Supramolecular assembly	—	2,4-Diamino-6-phenoxy-1,3,5-triazine	Porous nanosheets	CM-xphO	RhB and TC-HCl degradation	30
Top-down approaches	Chemical exfoliation	$K_2Cr_2O_7$–H_2SO_4	Dicyandiamide	Porous nanosheets	Porous g-C_3N_4	RhB degradation	38
		H_2SO_4 and HNO_3	Melamine	Porous ultrathin nanosheets	PUOCNs	Methyl orange degradation	39
	Thermal oxidation	—	Ammonium persulfate and melamine	Porous nanosheets	D-g-C_3N_4	Meropenem removal	40
			Urea and ammonium oxalate	Ultrathin porous layers	OPCN	Bisphenol A removal	41

carbon nitride interlayers and converted into chinone groups, finally forming porous structures.[38] Wan *et al.* prepared ultrathin g-C_3N_4 by dissolving BCN in concentrated H_2SO_4.[46] The rapid and intense heating effect caused by mixing water and H_2SO_4 caused the hydrogen bonds to break, forming ultrathin nanosheets, and the etching of H_2SO_4 resulted in the formation of porous structures. The pH of urea solution was adjusted with 0.1 M hydrochloric acid and ultrathin PCN nanosheets were obtained *via* exfoliation with isopropyl alcohol.[47] Acidification, drying and self-assembly could prompt the formation of gaps between the adjacent urea molecules. Besides, during urea condensation, abundant NH_3 and CO_2 gas bubbles are produced, which eventually burst. The stripping process between the acidified urea molecules is beneficial for the formation of a porous structure.[49] Besides, Zhou *et al.* synthesized ultrathin g-C_3N_4 nanosheets with hierarchical pores (P-mMCNNS) by calcining dicyandiamide and NH_4Cl in a nitrogen atmosphere.[50] The decomposition of NH_4Cl resulted in the formation of NH_3 and HCl, which can act as gas bubbles templates to form porous structure. Besides, a nitrogen atmosphere is beneficial for the production of macro–mesopores. Also, the hierarchical porous nanosheets showed fascinating photocatalytic performances, which was ascribed to their large surface area, multi-mass transport channels and short charge transfer distance (Fig. 2a).

Recently, supramolecular self-assembly has also gained increasing attention owing to the specificity and reversibility of hydrogen bonds, which are broken to form well-defined porous structures.[51] Melamine–cyanuric acid with hydrogen bonding is often used as a precursor to prepare PCN *via* supramolecular self-assembly.[30] The hydrogen bonding leads to the formation of a supramolecular complex, and the N atoms on the heptazine ring are substituted by C atoms to form a CN structure after polycondensation of the supramolecular complex (Fig. 2b). Moreover, the morphology and structure will change due to the steric hindrance of the substituents and heteroatoms. Liu *et al.* synthesized mesoporous g-C_3N_4 nanosheets utilizing a fresh supramolecular precursor.[52] The research proposed the formation of a melamine–cyanurate complex *via* hydrothermal treatment for dicyandiamide, and the complex was easily converted into PCN with ultrathin nanosheets *via* calcination. The bandwidth and photocatalytic activity of the prepared material were narrower and higher than that of PCN, respectively.

As is known, a large specific surface area is favorable for an enhancement in catalytic ability owing to the presence of more active reaction sites. The catalytic performance of most PCN is also unsatisfactory. Therefore, in this section, more morphology control strategies and methods are reviewed to obtain more satisfactory catalytic performances. These methods can shorten the charge migration distances and enlarge the multi-mass transport channels. In the future, more advanced methods and strategies to synthesize PCN should be explored to meet the demands of highly efficient catalytic performances.

2.2 Defect engineering

The presence of defects on the surface not only provides abundant active sites but also prevents the rapid recombination of photo-carriers. Considering the chemical

structure facilitates the separation of photo-induced carriers and extends the absorption edge. Many heteroatoms have been used to construct doped PCN and the doped metal elements can alter the morphology of PCN, which is beneficial to achieve morphology control. Therefore, the combined effect of doping engineering and morphology control engineering needs to be study further. Besides, computational modeling shows potential in this field. Combining DFT calculations or other computational modeling is worth studying for the development of doped PCN.

2.4 Hybridizing strategy

The hybridizing strategy is considered the most common and simplest method to promote surface charge separation. In general, the hybridizing strategy is achieved by coupling with a narrow-bandgap semiconductor and depositing a co-catalyst,[78] and these two ways result in different carrier separation mechanisms. When coupling with a semiconductor, a heterojunction will be constructed. Two semiconductors with an unequal band structure can be stimulated to produce photo-induced electrons, which can be transferred to avoid recombination. The relevant details were reviewed by Yu's group.[79] Usually, there are about three main forms of heterojunctions in coupling PCN with semiconductors, including conventional type-II heterojunctions, p–n heterojunctions, and Z-scheme heterojunctions. For example, a hierarchically porous type-II heterojunction was synthesized using zinc oxide (ZnO) and g-C_3N_4.[80] The photogenic electrons from the conduction band (CB) of g-C_3N_4 transferred to the CB of ZnO, while the photogenerated holes from the valence band (VB) of ZnO migrated to the VB of g-C_3N_4 under light irradiation, resulting in the separation of the electron–hole pairs. The composite showed high photodegradation activity for rhodamine B (RhB) and phenol. However, the enhanced electron–hole separation through the type-II heterojunction is not sufficient to overcome the ultrafast electron–hole recombination on the semiconductor. Thus, the p–n heterojunction has been proposed to accelerate the electron–hole migration and increase the photon-generated electron lifetime by providing an additional electric field. Li *et al.* proposed a p–n-type Bi_5O_7I-modified PCN heterojunction with excellent catalytic ability, which was nearly 30 times higher than that of pure g-C_3N_4.[81] However, in the above heterojunctions, both the reduction and oxidation processes occur at lower reduction and oxidation potentials, sacrificing the redox ability. Therefore, the Z-scheme heterojunction has been proposed to maximize the redox potential of the heterojunction systems. Lv *et al.* combined PCN with BiOBr to construct a Z-scheme heterojunction to restrain the recombination of photo-induced carriers.[82] The photogenic electrons from the CB of BiOBr were easily transferred to the VB of PCN. The transmission electron microscopy (TEM) images suggested that a BiOBr nanolayer was scattered over the surface of the PCN nanosheets, and 20% PCN/BiOBr showed the highest photocatalytic activity for the degradation of methylene blue (MB).

Conversely, when depositing a co-catalyst, the stability and selectivity of the main catalyst in the catalytic process are promoted.[83] Although the co-catalyst is an intrinsically inactive material, it can collect the photogenerated charge carriers and provide more active sites because of its superior conductivity or its ability to store electrons.[84] Briefly, the co-catalyst can prevent electron–hole recombination in the main catalyst. Co_3O_4 quantum dots as a co-catalyst were deposited on PCN *via* a facile annealing process to enhance its catalytic performance.[85] Because of the strong interaction, abundant pores were *in situ* produced during this process. More importantly, this work provided a new strategy for designing a co-catalyst on PCN. Besides, AuCu alloy nanoparticles (NPs) were used as a co-catalyst to modify ultrathin PCN nanosheets.[47] The light absorption was enhanced because of the local surface plasmon resonance (LSPR) of the Au NPs, which accelerated the C–C combination process in the production of ethanol. In addition, Chen *et al.* loaded ultrathin MoS_2 as a co-catalyst on PCN to enhance its photocatalytic performance.[86] The ultrathin MoS_2 extracted photo-induced electrons from g-C_3N_4 and increased the number of adsorption sites for RhB.

In conclusion, hybridizing semiconductors or co-catalyst is a mature strategy to suppress the recombination of charge carriers. Combining with semiconductors can regulate the band structure of composites and the electron transport path at the interface to enhance the separation of charge carriers. In addition, a co-catalyst can provide more active sites and trap photo-induced electrons to reduce charge carrier recombination. Besides, the specific characters of semiconductors and co-catalyst are also good for an improvement in the catalytic performance. Thus, the excellent catalytic ability of PCN shows its potential for application in water treatment.

2.5 Anchoring single atoms

Single atom catalysts, with maximum atom utilization, well-distributed active sites, and strong metal–support interactions, have become a new frontier in catalysis.[87,88] Although single dispersed atoms easily aggregate into large clusters, a suitable support can enhance the stability and dispersity of single-atom catalysts.[89] Porous 2D materials provide sufficient space and act as an excellent support to anchor single atoms.[90] Besides, g-C_3N_4 is also widely used to accommodate single atoms because its six-fold cavity can provide an ideal position.[91] Therefore, it is a research frontier for anchoring single atoms onto the PCN network *via* coordination bonds. For instance, Yang *et al.* reported an *in situ* growth strategy to implant single-atom cobalt in PCN.[92] The photocatalytic performance of the single-atom cobalt dispersed PCN was enhanced because the formed chemical bonds facilitate charge separation and transfer. Moreover, single-atom cobalt can efficiently increase the electron density and enhance the light absorption. The OTC degradation of Co(1.28%)–PCN was about 3.7 times that of

pristine PCN. Li *et al.* constructed a single-atom silver-incorporated g-C_3N_4 catalyst.[91] According to the density functional theory (DFT) calculations, single-atom silver was anchored in the six-fold cavity of g-C_3N_4, and the formed N–Ag bonding solved the issue of metal agglomeration at higher temperature. Particularly, this study proved that the Gibbs free energy of the intermediate state (ΔG_{H*}) increased because the pyridinic N atoms adjacent to Ag occupied the six-fold cavity, which was favorable for the hydrogen evolution reaction. This work developed a new strategy to design catalysts with ultrahigh photoactivity and photothermal stability. Zhao *et al.* anchored single-atom platinum (Pt) on holey ultrathin g-C_3N_4 nanosheets (Pt–CNHS) as cathode electrocatalysts for Li–O_2 batteries.[93] The synergism between single-atom Pt and CNHS enhanced the battery performance, such as providing excellent rechargeability and high specific capacity.

Compared with conventional metal nanoparticles, single-atom catalysts can achieve maximum atom-utilization efficiency to exhibit excellent stability and catalytic activity. The catalytic activity of single-atom catalysts is ascribed to the interaction between single atoms with the coordinating atoms on the support. The formation of strong bonds endows single atoms with stability, overcoming their high aggregation propensity. PCN with a porous structure and N-rich cavities is beneficial for anchoring single atoms. Especially, Li *et al.* proved that anchoring single-atom Ag on g-C_3N_4 can solve the aggregation problem at high temperature, which provides new guidance for the design of single-atom catalysts. Although anchoring single atoms is a new frontier in catalysis, the preparation of single atoms is difficult and improving their dispersibility is also a challenge. It is also necessary to investigate the structure and catalytic mechanism *via* theoretical calculations.

3. The application of FPCN in water treatment

According to the functional modification presented in section 2, PCN with a large surface area and unique energy band positions has gained wide attention for the treatment of environmental pollution. Its large surface provides abundant active sites in the reaction process to improve the mass transfer process. In addition, the unique electronic structure and adjusted energy band positions benefit the separation of charge carriers and promote the production of more active radicals for photocatalytic degradation reactions. Recently, more researchers have given attention to water disinfection and microbial control *via* the use of g-C_3N_4-based nanomaterials. In this part, we highlight the recent water treatment applications based on PCN.

3.1 Adsorption

Adsorption is a simple technique to remove heavy metals and organic pollutants in wastewater treatment, and it is widely used as a pretreatment approach for the large-scale elimination of contaminants.[6] In the adsorption process, strong surface complexes are generally formed owing to electrostatic attractions, H-bonding, pore-filling, hydrophobic effect, and π–π electron donor–acceptor coactions of organic molecules.[94] When the adsorption materials are added, the remaining pollutants will be quickly adsorbed on their surfaces, and then be further degraded. For example, Zhu's group proposed a novel nanoporous g-C_3N_4 (npg-C_3N_4), showing enhanced adsorption activity.[24] When the proportion of thiourea was about 80%, the surface area of npg-C_3N_4 was about 46.7 m^2 g^{-1} with a pore width of around 3.7 nm, which exhibited 40.0% MB adsorption from solution, as shown in Fig. 5a–c. Besides, a simple two-step thermal method was proposed by Liu and coworkers to synthesize porous ultrathin g-C_3N_4 nanosheets with carbon vacancies (Cv-CNNs).[7] This work firstly revealed the SDZ adsorption capability of Cv-CNNs by quantum mechanical simulations (Fig. 5d and e). The results indicated that the improved adsorption capability was ascribed to the synergy of the large surface area and carbon vacancies, which affected diverse levels of H saturation. Accordingly, the enhanced adsorption was beneficial for the elimination of low-concentration antibiotics, showing potential practical application for the degradation of micropollutants in water. Zhu's group fabricated a 3D g-C_3N_4/TiO_2 heterojunction, which exhibited enhanced adsorption efficiency and offered more active sites to shorten the mass transfer distance during the surface reaction.[95] The optimized surface area of 3D g-C_3N_4/TiO_2-57% was 9.8 times larger than that of BCN, while the MB adsorption (2.916 mg g^{-1}) was 10.5 times higher than that by BCN (Fig. 5f). The increase in the surface area of the 3D structure improved the MB adsorption ability.

Most heavy metals such as cadmium (Cd), zinc (Zn), copper (Cu), lead (Pb), and mercury (Hg) can be removed by adsorption, which affect the environmental system and pose a threat to living creatures. Moreover, it has been reported that trace levels of heavy metals exist in drinking water, including Cd (0.003 mg L^{-1}), Cu (2.0 mg L^{-1}), Pb (0.01 mg L^{-1}) and Hg (0.001 mg L^{-1}), causing significant health issues to humans.[96] In terms of heavy metal removal, the system conditions (*i.e.*, pH and surface functional groups) will affect the adsorption process. Specifically, solution pH can affect the surface charge of the prepared samples and heavy metal ion distribution, resulting in electrostatic interaction between the catalyst and contaminant.[97] Wang's group demonstrated that different pH affected the adsorption of Cr over calcined CoFe–LDH/g-C_3N_4.[98] At pH = 2.0, Cr(VI) was completely removed within 100 min. This was because the negatively charged Cr(VI) was adsorbed on the positively charged calcined 50%-CoFe–LDH/g-C_3N_4 under strong acidic condition. Besides, the hard ferrite nature of the composites with high remanence and coercivity (Fig. 5g) was beneficial for the separation of the composites from wastewater. Gu *et al.* fabricated an LS-C_3N_4/CWS catalyst consisting of lignosulfonate-functionalized g-C_3N_4 and carbonized wood

In addition, nitroaromatics have been proven to damage the aquatic environment and are difficult to completely remove owing to their strong stability and difficult biodegradation.[109] Catalytic reduction is considered an efficient method to reduce nitroaromatics. Although noble nanoparticles are widely used for the reduction of nitroaromatics, it is essential to choose suitable supports to immobilize these nanoparticles because of their high aggregation. The amine groups on the surface of PCN can anchor metal nanoparticles to enhance their dispersity, stability and catalytic activity.[110] Hence, PCN can be used for the reduction of nitroaromatics. For example, Qin *et al.* designed a PDA–g-C_3N_4/Au catalyst for the highly efficient reduction of nitroaromatics by $NaBH_4$.[110] The catalyst exhibited excellent catalytic activity with a rate constant of 0.0514 s^{-1} and turnover frequency (TOF) of545.60 h^{-1} for the reduction of 4-nitrophenol (4-NP). Hu *et al.* synthesized a 2D Rh/Fe_3O_4/g-C_3N_4–N compound, which showed an excellent catalytic performance towards the transformation of nitroarenes into relevant anilines in water *via* hydrogenation.[111] After 12 recycles, the catalytic property had an obvious decrease. This research provided a guide for the further catalytic reduction of various noble metals. Balakumar *et al.* fabricated S-doped g-C_3N_4 assembled by gold nanoparticles, and the obtained catalyst achieved the effective conversion of 4-nitrophenol in catalytic reduction.[112] It was reported that the catalytic efficiency obtained was near 100% within 5 min due to the fast electron transfer reduction.

FPCN shows potential in the removal of heavy metal ions and nitroaromatics from aqueous solutions, and the adjusted band gap of g-C_3N_4 advances the visible light absorption and charge carrier separation, which are vital for the catalytic reduction. In addition, in some research, organics can capture the photo-induced holes to improve the separation of photo-induced holes–electrons, which is beneficial for the photo-reduction of metal ions. Therefore, functional PCN materials show potential for the efficient elimination of metal ions and nitroaromatics through adsorption–catalytic reduction processes.

3.2.2 Removal of dyes. With the development of industrialization, dye wastewater has attracted significant attention, which brings a huge risk to the environment and human beings.[113] FPCN, which is obtained by inducing amino groups or defects in PCN, is beneficial for dye removal *via* physical adsorption or chemical interaction. For example, PCN showed excellent photo-degradation efficiency for the degradation of both the cationic MB and anionic methyl orange (MO), and $^{\bullet}O_2^-$ was found to play a primary role in the photodegradation.[114] Zhang *et al.* constructed a porous graphene aerogel-g-C_3N_4 (GA-g-C_3N_4) heterojunction with the purification capacity of 83.0% for MB within 3 h irradiation. The adsorption capacity towards dye was enhanced and the photo-induced electron–hole recombination was diminished on account of the combination to form a heterojunction, benefiting the photocatalytic performance.[115] Considering that the common g-C_3N_4 generally exhibits a negatively charged surface, it usually shows higher adsorption capacity for cationic dyes than anionic dyes.[116] Therefore, it is crucial to develop functional PCN catalysts with excellent degradation ability towards anionic dyes. An ultrathin PCN material with surface carbon defects exhibited 96.2% RhB degradation efficiency.[117] The main active species in the RhB photo-reduction system changed from $^{\bullet}O_2^-$ over BCN to both $^{\bullet}O_2^-$ and $^{\bullet}OH$ over the ultrathin PCN. Zhao *et al.* demonstrated an electrophoretic deposition method to deposit PCN/reduced graphene oxide (rGO) on nickel (Ni) foam (CNG–Ni) to form a highly active CNG–Ni foam photoanode.[100] CNG–Ni showed synergy between RhB removal and H_2 evolution. RhB could serve as a sacrificial agent to capture photogenerated holes, resulting in more photo-induced electrons transferring to the cathode for H_2 evolution (Fig. 7a). During the PEC process, CNG–Ni exhibited potential in pollutant control and energy generation. Shen *et al.* prepared P, K-co-doped PCN in a vapor and self-producing NH_3 atmosphere.[118] The XPS spectra revealed the substitution of the C position by P atoms in g-C_3N_4, while the K atoms may be combined with N or C to form a new bridge (K–N and K–C, respectively) (Fig. 7b). The bandgap and electronic structure were adjusted on account of the change in electron density around the C and N atoms. The bandgap energies (Fig. 7c) and XPS valence band (Fig. 7d) indicated that the P, K-co-doped g-C_3N_4 showed a high valence band and low bandgap energy, meaning a high oxidation capacity, outstanding visible-light availability and charge excitation. Fig. 7e shows that the photocatalytic performances of P, K-co-doped g-C_3N_4 for RhB elimination distinctly improved, which is ascribed to its large surface area, lower bandgap energy and lower recombination rate of photogenic carriers.

PCN showed excellent degradation efficiency for dye in many studies. Light can reflect and scatter from the nanoporous interiors of PCN. In addition, its large surface area can provide abundant catalytic active centers and visible light harvesting, which are crucial for dye degradation *via* AOPs.

3.2.3 Removal of other organics. The cumulative concentration of pharmaceuticals and personal care products (PPCPs) in the environment has caused adverse effects on human health and natural ecosystems.[119,120] Therefore, abundant methods have been developed to remove PPCPs. PCN has been widely used in AOPs to achieve efficient PPCP removal. For example, Liang *et al.* proposed carbon quantum dot-modified PCN to remove diclofenac (DCF) *via* photocatalysis.[11] DCF, as the most popular non-steroidal anti-inflammatory drug (NSAIDs), is extensively used.[121] However, it has been reported that traces DCF at the concentration level of about μg L^{-1} and ng L^{-1} in the environment has adverse effects towards human health and the ecosystem due to its low biodegradability.[122] In this study, DCF was finally degraded by ring hydroxylation, ring closure and C–N bond cleavage (Fig. 8a and b). Wu *et al.* synthesized carbon dot/g-C_3N_4 hollow porous nanospheres (HCNS/CDs), which exhibited enhanced solar-light-driven PPCP remediation, especially for the removal of naproxen

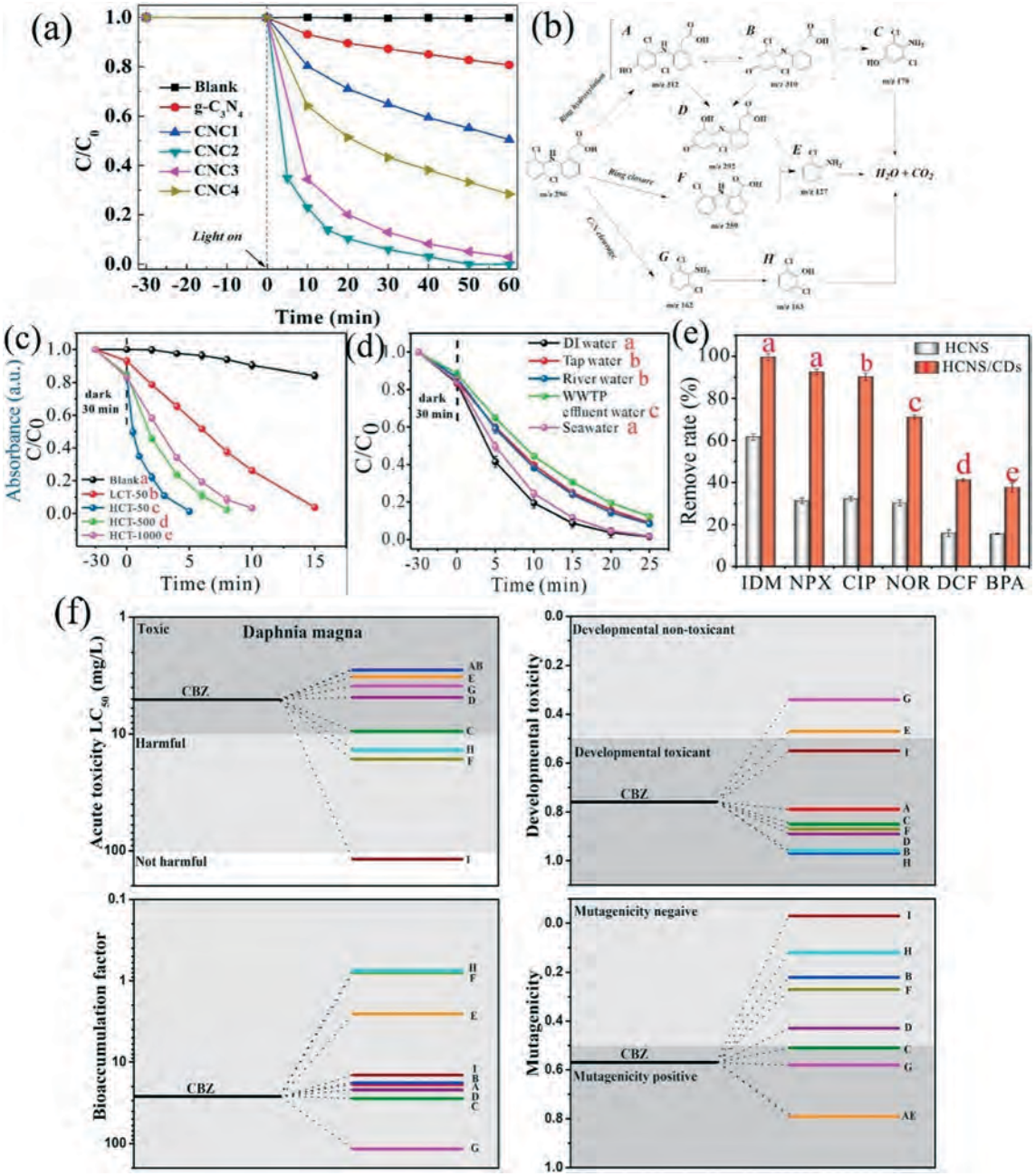

Fig. 8 Degradation kinetics (a) and degradation pathway (b) of DCF by various photocatalysts. Adapted from ref. 11 with permission from Elsevier, Copyright 2019. (c) Photocatalytic activity of HCNS/CDs based on the degradation of NPX. (d) Photodegradation of NPX with HCNS/CDs in different water matrices. (e) Photocatalytic degradation of PPCPs by HCNS and HCNS/CDs under visible light irradiation. Adapted from ref. 3 with permission from Elsevier, Copyright 2020. (f) Toxicity assessment. Adapted from ref. 125 with permission from Elsevier, Copyright 2020.

surface water sources, ground waters, and even drinking water sources, while it is up to 2 mg L^{-1} in livestock wastewater.[132] Porous noble-metal-free co-doped g-C_3N_4 (C/Ce–CN) was synthesized *via* supramolecular self-assembly to degrade TC.[133] The TC photocatalytic removal efficiency over C/Ce–CN was about 2.6 times superior to that of pristine CN. The photoelectrical test (Fig. 9a–d) revealed that C/Ce–CN exhibited a faster charge transfer rate and longer carrier lifetime. Yang *et al.* fabricated ultrathin PCN decorated with boron nitride quantum dots, which degraded oxytetracycline hydrochloride (OTC-HCl) *via* intensive exaction dissociation and charge transfer.[134] Therefore, it provided new insight to explore highly efficient and stable composites.

Additionally, CN-based materials have also been used to remove many phenolic pollutants. Phenol-contaminated wastewater is high-toxicity industrial wastewater and is refractory to remove with a concentration in the range of 20 to 1200 mg L^{-1}.[135] For the degradation of phenol, a hierarchical PCN foam photocatalyst with nano-scale (~50 nm) and micron-(1–2 μm) pores was synthesized. The reagents and products

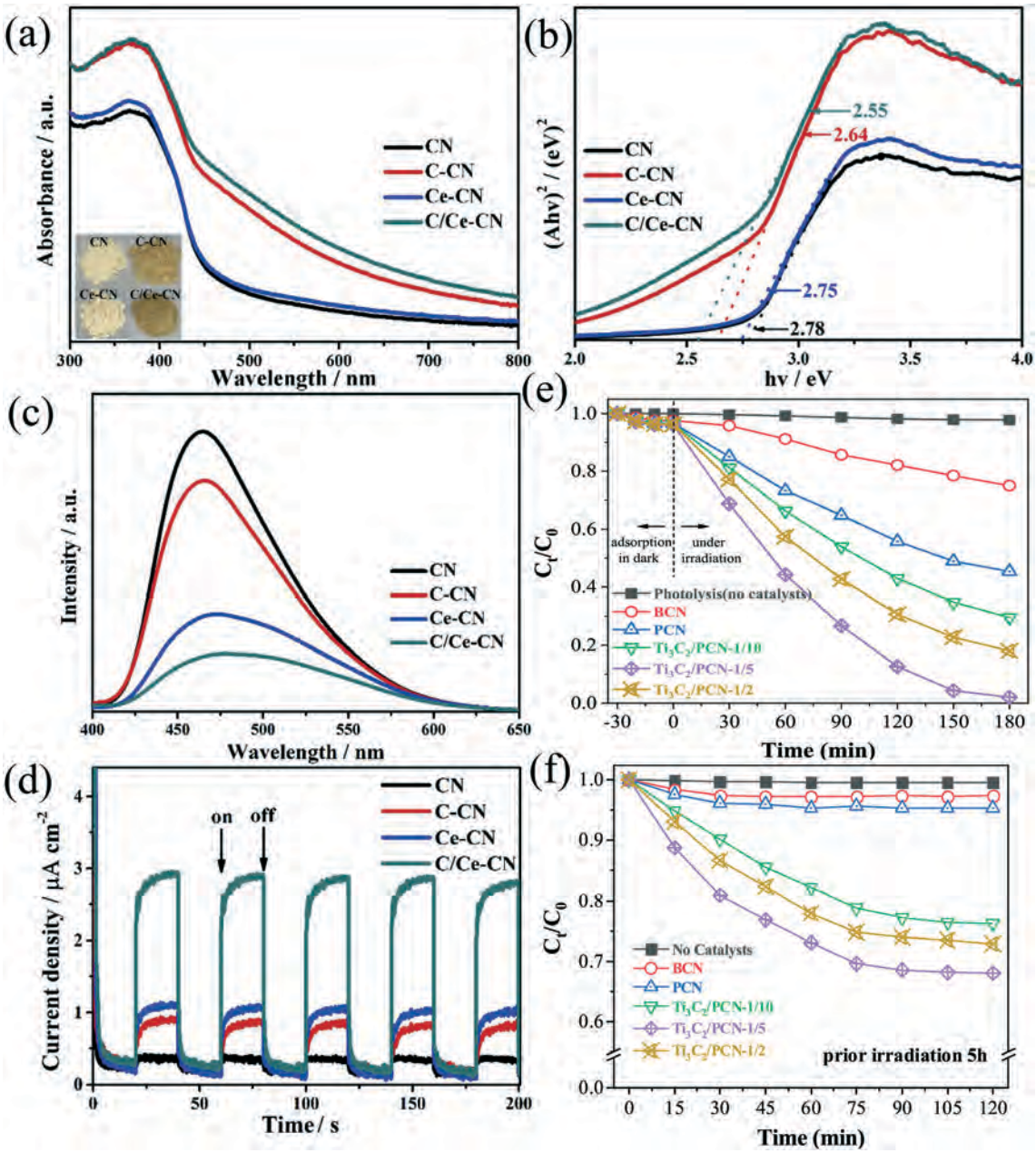

Fig. 9 (a) UV-DRS (photograph of the samples shown in the inset), (b) energy gap, (c) photoluminescence emission spectra, and (d) transient photocurrents response of CN and modified CN. Adapted from ref. 133 with permission from Elsevier, Copyright 2020. (e) Day-photocatalytic degradation and (f) night-photocatalytic degradation of phenol. Adapted from ref. 137 with permission from Elsevier, Copyright 2020.

moved freely in the inner pores to improve the mass transfer, finally resulting in the degradation of 93.4% phenol within 180 min.[136] Liu *et al.* synthesized a 2D/2D Ti_3C_2/PCN van der Waals (VDW) heterostructure photocatalyst to remove phenol.[137] The photocatalytic ability of Ti_3C_2/PCN was available during both day and night. The phenol removal efficiency reached 98% over Ti_3C_2/PCN in the day-photocatalytic work (Fig. 9e) due to the enhanced absorbing visible light of the PCN nanolayers and the built-in electric field of the VDW heterojunction. Besides, 32% of phenol was decomposed in the dark (Fig. 9f) due to the presence of Ti_3C_2, which could store extra photo-induced electrons from visible light illumination and release them when exposed to electron acceptors. Furthermore, Ti_3C_2/PCN exhibited the universal applicability and could degrade various organic contaminants. Gao *et al.* fabricated oxygen-doped graphitic carbon nitride (O–CN) with long-term stability for PMS activation toward the degradation of bisphenol A.[138] The electronic structure was modulated to benefit the production of $^1O_2$, contributing to the highly selective reactivity of the O–CN/PMS system. Also, the properties of PCN applied in the removal of organics are presented in Table 2. The research on the removal of organics is rich, comprehensive, and instructive. In the future, we should focus of applying these technologies for practical sewage treatment.

Table 2 Summary of the performance of PCN catalysts for the removal of organics

Organics	Concentration	Catalysis	Characters	Methods	Degradation rate	Ref.
Diclofenac (DCF)	μg L^{-1} or ng L^{-1}	CQDs/PCN	Hybridizing strategy	Photocatalysis	0.074 min^{-1} 96.1%/60 min	11
Naproxen (NPX)	0.1 ng L^{-1} to 7.69 μg L^{-1}	HCNS/CDs	Hybridizing strategy	Photocatalysis	0.1603 min^{-1} 98.6%/25 min	3
Carbamazepine (CBZ)	ng L^{-1} to μg L^{-1}	$NiCo_2O_4$/g-C_3N_4	Hybridizing strategy	PMS/photocatalysis	0.3956 min^{-1} 99.0%/10 min	125
Sulfamethoxazole (SMX)	ng L^{-1} to μg L^{-1}	pNS g-C_3N_4	Morphology control	Photocatalysis	0.085 min^{-1} 93.39%/30 min	127
		S–C_3N_4/C-dot	Doping engineering	Photocatalysis	90%/180 min	139
Indometacin (IDM)	5–792 ng L^{-1}	COCN	Doping engineering	Photocatalysis	0.0391 min^{-1}	128
Tetracycline (TC)	Hundreds μg L^{-1}	CNx	Defect engineering	PS/photocatalysis	0.3475 min^{-1}	140
		Ag/PCN	Hybridizing strategy	Photocatalysis	0.0120 min^{-1} 83%/120 min	141
		NDCN–S	Doping engineering	Photocatalysis	81.72%/60 min	142
		C/Ce–CN	Doping engineering	Photocatalysis	0.04027 min^{-1} 90.1%/60 min	133
Tetracycline hydrochloride (TCH)	ng L^{-1}	Fe-POM/CNNS-Nvac	Doping/defect engineering	Fenton-like	0.1520 min^{-1} 95.5%/18 min	104
Oxytetracycline (OTC)	ng L^{-1}	Co/pCN	Anchoring single atom	Photocatalysis	0.038 min^{-1} 75.7%/40 min	92
Oxytetracycline hydrochloride (OTC-HCl)	ng L^{-1}	BNQDs/UPCN	Hybridizing strategy	Photocatalysis	0.0309 min^{-1} 82%/60 min	134
Phenol	20 to 1200 mg L^{-1}	Hierarchical PCN	Morphology control	Photocatalysis	93.4%/180 min	136
		Ti_3C_2/PCN	Hybridizing strategy	Photocatalysis	0.022 min^{-1} 98%/180 min	137
Bisphenol A (BPA)	30 to 412 ng L^{-1}	O–CN	Doping engineering	PMS activation	100%/45 min	138

3.3 Leachate control

Leachate, which is caused by the ultimate treatment of abundant industrial and municipal solids, consists of heavy metals, ammonia–nitrogen compounds, refractory and toxic organic compounds.[143,144] Once high-concentration leachates are released into the environment without strict treatment, they pose a hazard to surface and subsurface water and even threaten human health.[145] Therefore, it is vital to carefully treat liquid leachates before their release into the surroundings. AOPs, with high reactivity and low environmental risk, have been considered as potential and efficient methods for the treatment of leachates.[146–148] There are various RS induced by AOPs, such as $^{\bullet}OH$, $O_2^{\bullet-}$, $SO_4^{\bullet-}$ and $^1O_2$, which can efficiently degrade organic chemicals.[149] Considering that TiO_2 combined with AOPs has been proven to be an efficient method to treat leachates,[150] exploring alternative semiconductor photocatalysts to treat leachates has been a research hotspot. Considering the high photosensitivity and suitable electronic structure of PCN, it is possible to substitute TiO_2, which is becoming a rising catalyst in leachate control. However, the application of PCN in AOPs is rare, and here we present our best effort to review the existing research. Hu *et al.* demonstrated a method of immobilizing *P. chrysosporium* on a g-C_3N_4 photocatalyst to degrade organics in landfill leachates.[151] The obvious mesoporous sheet structure of g-C_3N_4 was beneficial for the carrier transfer and photocatalytic reaction. TOC removal was improved *via* the photocatalytic process of g-C_3N_4 and the biosorption and biodegradation process of *P. chrysosporium*. Besides, according to Fig. 10, almost all the organics in the landfill leachate, particularly the long-chain hydrocarbons and volatile fatty acids, could be eliminated by the immobilized *P. chrysosporium* under illumination. Therefore, immobilizing *P. chrysosporium* on the g-C_3N_4 catalyst shows potential for the treatment of landfill leachates. In addition, it is vital to improve the nitrate reduction in leachates. The intimate coupling of photocatalysis and biodegradation (ICPB) proposed by Zhang *et al.* not only could degrade bio-recalcitrant pollutants but also led to nitrate reduction.[152] After 16 h, the nitrate removal rate was up to 40.3% due to the synergy of the effect of *in situ* formed biofilms and photocatalysis over TiO_2/g-C_3N_4. Firstly, nitrate was reduced to nitrite under the effect of the biofilms. Then the production of N_2 improved because nitrite was further reduced *via* the synergy between the photocatalyst and biofilms. Therefore, an efficient method was proposed for the reduction of nitrate. However, considering the complex ingredients of leachates in practical conditions, PCN as a remediator in leachate treatment still needs development, and the relevant reported studies is fragmented. However, the mechanisms of PCN to eliminate the contaminants in leachate are adequate. Thus, combining AOPs with PCN shows potential for the treatment of refractory pollutants in leachates.

3.4 Constructing membrane systems

In actual wastewater treatment, it is challenging to recycle the catalyst, resulting in high cost and second pollution. Accordingly, membrane separation is known as an effective method without secondary pollution for wastewater purification, where the membrane is must competent for the

improve their drinking water sources, suffering a high risk of infections from pathogenic microorganisms. Therefore, it is crucial to control microorganisms in drinking water.[160] Heterogeneous photocatalysis, which can generate electron–hole pairs and highly RS *via* semiconductor activation, makes pathogen inactivation possible[161,162] by damaging essential macromolecules and has been anticipated to be a next-generation sustainable method to purify water. More specifically, photocatalysis based g-C_3N_4 is considered efficient and green technology for water disinfection due to its low cytotoxicity,[26] and antibacterial[27] and antiviral[28] activity. FPCN has been used as a bactericide to inactivate *Escherichia coli* (*E. coli*),[163,164] *Staphylococcus aureus* (*S. aureus*),[165] *Bacillus anthracis* (*B. anthracis*),[166] and *Salmonella*.[167] For example, Zhu's group synthesized a porous g-C_3N_4 nanosheet (PCNS) composite *via* a simple two-step template-free strategy.[164] PCNS possessed abundant surface-active sites to enhance charge transfer, and therefore the *E. coli* cells were completely inactivated over PCNS within 240 min while the removal rate of *E. coli* was only 77.1% by BCN (Fig. 11a). Fig. 11b–g further demonstrate the removal of *E. coli* by images and TEM analysis.

Kang *et al.* demonstrated a facile bacterial liquid exfoliation approach to exfoliate BCN into thin slices using active bacteria (Fig. 12a).[168] According to the morphology analysis, the surface area of the bacteria-treated 2D g-C_3N_4 (BT-CN-2d) composites increased to 82.61 $m^2\ g^{-1}$ with an in-plane porous structure (Fig. 12b–d). Fig. 12e shows that the *E. coli* were completely killed within 120 min over BT-CN-2d, and Fig. 12f shows that ROS in low concentration was

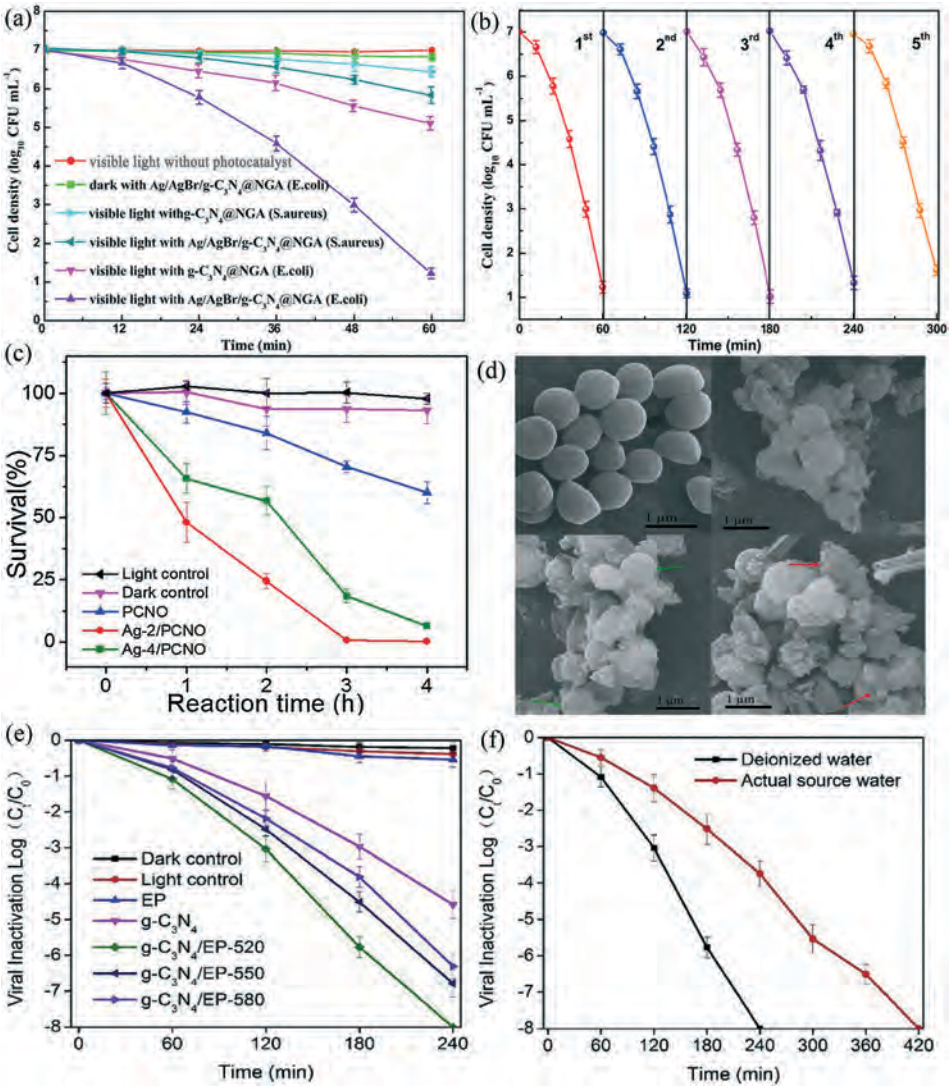

Fig. 13 (a) Disinfection performance for *E. coli* and *S. aureus* over different catalysts. (b) Cycle test of Ag/AgBr/g-C_3N_4@NGA for *E. coli* under visible light for five continuous operation. Adapted from ref. 165 with permission from Elsevier, Copyright 2019. (c) Photocatalytic disinfection activity for *S. aureus* with PCNO and Ag/PCNO. (d) SEM images of *S. aureus* cells after different treatment times. Adapted from ref. 170 with permission from Elsevier, Copyright 2019. (e) Photocatalytic MS_2 inactivation. (f) Effect of water matrix on viral inactivation with g-C_3N_4/EP-520. Adapted from ref. 172 with permission from Elsevier, Copyright 2018.

insufficient to cause bacterial damage. Chen *et al.* prepared a 3D porous silver/silver bromide/g-C_3N_4@nitrogen-doped graphene aerogel (Ag/AgBr/g-C_3N_4@NGA) composite.[165] Fig. 13a shows that the antibacterial property over Ag/AgBr/g-C_3N_4@NGA on *E. coli* and *S. aureus* were better than that of g-C_3N_4@NGA. The boosted antibacterial efficiency was ascribed to the formation of a Z-scheme heterojunction between g-C_3N_4 and AgBr. After several recycles, the catalysis still exhibited excellent antibacterial efficiency (Fig. 13b). However, the thicker cell wall composed peptidoglycan layers of *S. aureus*, a Gram-positive bacterium, was less sensitive to Ag/AgBr/g-C_3N_4@NGA.[165,169] Therefore, the inactivation efficiency of *S. aureus* was lower that of *E. coli* under similar conditions. An oxidized PCN loaded with Ag nanoparticles (Ag/PCNO) was used to inactivate *S. aureus*.[170] Because of the SPR and synergistic effects, 99.4% of the *S. aureus* cells were killed with Ag-2/PCNO after 3 h of irradiation (Fig. 13c). The scanning electron microscopy (SEM) analysis (Fig. 13d) proved that the *S. aureus* cells were embedded in Ag-2/PCNO and became malformed, even exhibiting some big cavities on the cell surfaces, indicating the inactivation of *S. aureus*. Urea-derived g-C_3N_4 (u-g-C_3N_4) with in-plane pores was used to fabricate photoactive, antimicrobial films to improve the antimicrobial activity.[166] The inactivation efficiency against *S. aureus*, methicillin-resistant *S. aureus* and *E. coli* O157 : H7 improved approximately 10-fold compared to their previous work.[171] Additionally, u-g-C_3N_4 was also demonstrated to deactivate *B. anthracis* endospores. Wang *et al.* proposed vanadate quantum dot-interspersed g-C_3N_4 (vanadate QDs/g-C_3N_4) with chiffon-like ripples and wrinkle porous structure.[167] The inactivation of *Salmonella* over $AgVO_3$ QDs/g-C_3N_4 reached up to 96.4% within 10 min under visible-light illumination, while g-C_3N_4 showed only 54.13% bactericidal efficiency under the same conditions.

Besides, g-C_3N_4-based materials are also used as viricides and algaecides. The risk of illness from viral pathogens is higher than that of bacterial pathogens; therefore, it is important to inactivate viruses. The size and structure of bacteriophage MS_2 is similar to many human pathogenic enteric viruses including easy propagation and non-pathogenicity to humans,[28,172] and thus it was selected as a model virus in a study. Zhang *et al.* developed a sustainable water-surface-floating composite by integrating g-C_3N_4 and expanded perlite (g-C_3N_4/EP).[172] The high specific surface area could optimize the performance for MS_2 disinfection, which achieved 8 log inactivation of MS_2 within 4 h visible-light irradiation without stirring (Fig. 13e). Importantly, in a real water source, g-C_3N_4/EP-520 showed excellent MS_2 inactivation, demonstrating its high efficiency for water disinfection (Fig. 13f). Besides, microalgae such as cyanobacteria pose a threat to drinking water because of their potential to cause algal blooms and release toxic metabolites in eutrophic lakes. It was reported that a g-C_3N_4/TiO_2 floating photocatalyst could remove *Microcystis aeruginosa* (*M. aeruginosa*) and *microcystin-LR* under visible light irradiation. During the degradation of *M. aeruginosa*, *microcystin-LR* was released into the water. g-C_3N_4/TiO_2 not only removed *M. aeruginosa* but also made *microcystin-LR* undetectable.[173] Z-scheme g-C_3N_4–MoO_3 (Mo–CN) photocatalysts with a mesoporous structure were proven to be beneficial for the surface adsorption of algal cells. In addition, h^+ and $^{\bullet}OH$ radicals made around 97% algal cells inactivate within 3 h visible light irradiation.[174] Composite-expanded perlite (*i.e.*, EP/Al_2O_3) deposited with g-C_3N_4 could also make *M. aeruginosa* inactivate, and *in situ* remediation driven by visible light showed potential for the control of cyano-harmful algal blooms (HABs) in aquatic systems.[175] Xu *et al.* proposed highly active $BiVO_4$/g-C_3N_4 nanosheet heterojunction photocatalysts to remove *microcystin-LR* (MC-LR).[176] The large surface area and

Table 3 Summary of the performance of PCN catalysts for water disinfection and microbial control

Catalyst	Target microorganism	Catalyst dose (g L^{-1})	Microbial level	Reaction time (min)	Inactivation performance	Ref.
PCNS	*E. coli*	0.4	5×10^6 CFU mL^{-1}	240	Complete inactivation	164
PCNS	*E. coli K-12*	0.4	6.5×10^6 CFU mL^{-1}	120	6.5 log inactivation	177
Ag/AgBr/g-C_3N_4@NGA	*E. coli*	0.268	1×10^7 CFU mL^{-1}	60	6 log inactivation	165
	S. aureus	0.268	1×10^7 CFU mL^{-1}	60	1.2 log inactivation	
V_N-PCN	*E. coli*	4	1×10^6 CFU mL^{-1}	120	4.8 log inactivation	178
	S. aureus	4	1×10^6 CFU mL^{-1}	120	4.24 log inactivation	
Ag/mpg-CN	*E. coli*	0.1	1×10^6 CFU mL^{-1}	180	80% inactivation	179
Fe_3O_4/Pd/mpg-C_3N_4	*E. coli*	0.1	1×10^8 CFU mL^{-1}	120	99.9% inactivation	180
	S. aureus	0.1	1×10^8 CFU mL^{-1}	120	99.8% inactivation	
Ag/PCNO	*S. aureus*	0.2	1×10^7 CFU mL^{-1}	180	99.4% inactivation	170
$AgVO_3$/g-C_3N_4	*Salmonella*	0.75	1×10^7 CFU mL^{-1}	10	7 log inactivation	167
g-C_3N_4/EP	*E. coli*	0.6	1×10^8 CFU mL^{-1}	180	8 log inactivation	172
	MS_2	0.6	1×10^8 CFU mL^{-1}	240	8 log inactivation	
g-C_3N_4	MS_2	0.15	1×10^8 PFU mL^{-1}	360	Complete inactivation	28
g-C_3N_4/TiO_2	*M. aeruginosa*	2	2.7×10^6 cells/mL	360	88.1%	173
	Microcystin-LR	2	50 μg L^{-1}	360	54.4%	
Mo–CN	*M. aeruginosa*	0.15	2.7×10^6 cells per mL	360	97%	174
Floating g-C_3N_4	*M. aeruginosa*	2	2.7×10^6 cells per mL	360	74.4%	175
$BiVO_4$/g-C_3N_4	*Microcystin-LR*	0.5	5 mg L^{-1}	10	100%	181
Ag_2O/g-C_3N_4	*M. aeruginosa*	0.05	4.78×10^6 cells per mL	360	99.94%	182

abundant mesopores of g-C_3N_4 provided an excellent contact area for $BiVO_4$. MC-LR (5 mg L^{-1}) was obviously eliminated within 10 min. The synergy between the abundant mesoporous structures and the interface Z-scheme heterojunction accelerated photo-induced electron–hole separation, benefiting the removal of MC-LR. Also, the properties of PCN applied to eliminate bacteria, viruses and algae are presented in Table 3.

In this section, the applications of PCN materials in the removal of bacteria, viruses, and algae were reviewed. Because PCN can generate highly RS *via* visible light activation, it is anticipated to be efficient for water disinfection and microbial control. However, research is mainly concentrated on the inactivation of bacteria, especially for *E. coli* and *S. aureus*. The study of the inactivation of other bacteria, viruses, and algae is still in its infancy. Besides, there are few studies for water disinfection and microbial control *via* other AOPs besides photocatalysis, which can also achieve water disinfection in theory. Therefore, there are plenty aspects that need to be explored for water disinfection with PCN.

4. Conclusions and prospects

PCN, with a large surface area, strong electron transport ability, and low cytotoxicity is an excellent catalyst for water treatment. On account of modifying PCN, its morphology and electronic structure can be adjusted to provide more reaction sites and suppress the recombination of charge carriers. For example, ultrathin nanosheets can shorten charge the migration distances and accelerate the carrier transfer compared with the bulk structure. The presence of defects on the surface can trap photo-induced electrons and prevent the rapid recombination of photo-carriers. In addition, carbon vacancies can enhance its visible light absorption. Doping heteroatoms can extend its absorption edge and inhibit the electron–hole recombination. Nonmetallic atoms may replace the sites of C or N, which alter the atomic arrangement and molecular orbital distribution, benefiting the separation of photo-induced carriers and extending the absorption edge. Metal atoms are easily captured in the in-planar cavity of g-C_3N_4 due to the strong interactions between the nitrogen pots and metal cations. Doping metals can narrow the energy gap, accelerate the charge mobility and alter the morphology. The hybridizing strategy has been proved to be an efficient method to transfer charge carriers and suppress their recombination. Anchoring single atoms can achieve maximum atom-utilization efficiency and improve stability to enhance the catalytic performance. These modifications make PCN show extensive potential in wastewater treatment. Herein, firstly, we reviewed the primary application of FPCN in wastewater treatment, such as the adsorption and degradation for heavy metal ions, dyes, and other organics. These applications provide fundamental guidance for other studies. In addition, the control for landfill leachate with FPCN was also reviewed, providing potential for complex ingredient removal in actual water bodies. Furthermore, to realize catalyst recycling and reduce the possible influence on the environment, constructing membranes with PCN was discussed to treat pollutants. Finally, FPCN applied in water disinfection microbial control was discussed, which is closely related to drinking water safety.

Although many efforts have been focused on PCN with excellent catalytic performances, there are still some challenges with PCN, ranging from its preparation to application. Notably, it is necessary to focus on the design and optimization of PCN to meet practical application demands. The specific aspects are summarized as follows:

1. The highly ordered mesopores and specific structure of PCN can generate abundant active sites comprised of low-coordinated atoms in defect sites, but the related green synthesis methods are still in their infancy. Especially, doping heteroatoms may affect the morphology of PCN to further enhance its catalytic performance. Therefore, it is also necessary to research multiple modification strategies.

2. The research on theoretical calculations is the trend of future development. Theoretical calculations can explain the electronic band structures and reaction mechanisms *via* molecular simulations and reaction kinetics, which can provide a guide for the design of catalysts and their modification. The theoretical calculation on PCN is still in its infancy and full of challenge.

3. In particular, most of the current research on PCN focused on adsorption and photocatalysis/photoelectrocatalysis due to its large surface area and excellent photoelectric property. However, the research on the application of PCN in other AOPs is rare and needs deeper exploration. Especially, some new systems, such as single-atom catalysts, have been proposed recently and need further development.

4. The other applications, such as leachate control and constructing membrane systems, are in their infancy. The control of leachates is related to daily life, and thus the development of efficient technologies is imperative. Constructing membrane systems is convenient for sample recycle and coupling with other physical or biological technologies to achieve higher degradation. Also, it is necessary to further explore the relevant applications.

5. In water disinfection and microbial control, the research mainly concentrated on the photo-inactivation of bacteria, especially for *E. coli* and *S. aureus*. The study of the inactivation of other bacteria, viruses and algae needs further development. Besides, in a previous report, photocatalysis-based PCN was used to degrade bacteria. However, we speculated whether the combination of photocatalysts and bacteria can also remove pollutants, which offer new insight for further research.

6. It is also necessary to analyze the possible impact on the environment. Although PCN has low cytotoxicity, the poisoning of hybridized PCN catalysts still deserves more attention. Besides, toxicity analysis of intermediates in the degradation process is also worth discussing to avoid potential risks.

In conclusion, this review summarized the development of PCN from its modification to application, presenting insight for the design and application of PCN in a new field. We hope this review will be a guide for the design of desired catalysts in the future.

Conflicts of interest

The authors declare that they have no known competing financial interests or personal relationships that could have appeared to influence the work reported in this paper.

Acknowledgements

This study was financially supported by the Program for the National Natural Science Foundation of China (U20A20323, 51521006, 51879101, 51579098, 51779090, 51909084), the National Program for Support of Top-Notch Young Professionals of China (2014), the Program for Changjiang Scholars and Innovative Research Team in University (IRT-13R17), Hunan Natural Science Foundation (2020JJ3009), Hunan Researcher Award Program (2020RC3025), the Fundamental Research Funds for the Central Universities (531119200086, 531118010114, 541109060031, 531118040083), the Hunan Provincial Innovation Foundation for Postgraduate (CX20190260) and the Three Gorges Follow-up Research Project (2017HXXY-05).

References

1 H. Wang, H. Wang, Z. Wang, L. Tang, G. Zeng, P. Xu, M. Chen, T. Xiong, C. Zhou, X. Li, D. Huang, Y. Zhu, Z. Wang and J. Tang, Covalent organic framework photocatalysts: structures and applications, *Chem. Soc. Rev.*, 2020, **49**, 4135–4165.

2 Y. Yang, X. Li, C. Zhou, W. Xiong, G. Zeng, D. Huang, C. Zhang, W. Wang, B. Song, X. Tang, X. Li and H. Guo, Recent advances in application of graphitic carbon nitride-based catalysts for degrading organic contaminants in water through advanced oxidation processes beyond photocatalysis: A critical review, *Water Res.*, 2020, **184**, 116200.

3 Y. Wu, F. Wang, X. Jin, X. Zheng, Y. Wang, D. Wei, Q. Zhang, Y. Feng, Z. Xie, P. Chen, H. Liu and G. Liu, Highly active metal-free carbon dots/g-C3N4 hollow porous nanospheres for solar-light-driven PPCPs remediation: Mechanism insights, kinetics and effects of natural water matrices, *Water Res.*, 2020, **172**, 115492.

4 J. He, C. Lai, L. Qin, B. Li, S. Liu, L. Jiao, Y. Fu, D. Huang, L. Li, M. Zhang, X. Liu, H. Yi, L. Chen and Z. Li, Strategy to improve gold nanoparticles loading efficiency on defect-free high silica ZSM-5 zeolite for the reduction of nitrophenols, *Chemosphere*, 2020, **256**, 127083.

5 H. Wang, X. Yuan, H. Wang, X. Chen, Z. Wu, L. Jiang, W. Xiong and G. Zeng, Facile synthesis of Sb2S3/ultrathin g-C3N4 sheets heterostructures embedded with g-C3N4 quantum dots with enhanced NIR-light photocatalytic performance, *Appl. Catal., B*, 2016, **193**, 36–46.

6 J. Jin, S. Li, X. Peng, W. Liu, C. Zhang, Y. Yang, L. Han, Z. Du, K. Sun and X. Wang, HNO3 modified biochars for uranium (VI) removal from aqueous solution, *Bioresour. Technol.*, 2018, **256**, 247–253.

7 M. Liu, D. Zhang, J. Han, C. Liu, Y. Ding, Z. Wang and A. Wang, Adsorption enhanced photocatalytic degradation sulfadiazine antibiotic using porous carbon nitride nanosheets with carbon vacancies, *Chem. Eng. J.*, 2020, **382**, 123017.

8 Y. Yu, W. Xu, J. Fang, D. Chen, T. Pan, W. Feng, Y. Liang and Z. Fang, Soft-template assisted construction of superstructure TiO2/SiO2/g-C3N4 hybrid as efficient visible-light photocatalysts to degrade berberine in seawater via an adsorption-photocatalysis synergy and mechanism insight, *Appl. Catal., B*, 2020, **268**, 118751.

9 S. Yang, Q. Li, L. Chen, Z. Chen, B. Hu, H. Wang and X. Wang, Synergistic removal and reduction of U(VI) and Cr(VI) by Fe3S4 micro-crystal, *Chem. Eng. J.*, 2020, **385**, 123909.

10 H. Yi, M. Yan, D. Huang, G. Zeng, C. Lai, M. Li, X. Huo, L. Qin, S. Liu, X. Liu, B. Li, H. Wang, M. Shen, Y. Fu and X. Guo, Synergistic effect of artificial enzyme and 2D nano-structured Bi2WO6 for eco-friendly and efficient biomimetic photocatalysis, *Appl. Catal., B*, 2019, **250**, 52–62.

11 W. Liu, Y. Li, F. Liu, W. Jiang, D. Zhang and J. Liang, Visible-light-driven photocatalytic degradation of diclofenac by carbon quantum dots modified porous g-C3N4: Mechanisms, degradation pathway and DFT calculation, *Water Res.*, 2019, **151**, 8–19.

12 R. A. Rather and I. M. C. Lo, Photoelectrochemical sewage treatment by a multifunctional g-C3N4/Ag/AgCl/BiVO4 photoanode for the simultaneous degradation of emerging pollutants and hydrogen production, and the disinfection of E. coli, *Water Res.*, 2020, **168**, 115166.

13 L. Li, C. Lai, F. Huang, M. Cheng, G. Zeng, D. Huang, B. Li, S. Liu, M. Zhang, L. Qin, M. Li, J. He, Y. Zhang and L. Chen, Degradation of naphthalene with magnetic bio-char activate hydrogen peroxide: Synergism of bio-char and Fe-Mn binary oxides, *Water Res.*, 2019, **160**, 238–248.

14 Z. Wang, C. Lai, L. Qin, Y. Fu, J. He, D. Huang, B. Li, M. Zhang, S. Liu, L. Li, W. Zhang, H. Yi, X. Liu and X. Zhou, ZIF-8-modified MnFe2O4 with high crystallinity and superior photo-Fenton catalytic activity by Zn-O-Fe structure for TC degradation, *Chem. Eng. J.*, 2020, **392**, 124851.

15 X. Zhou, Z. Zeng, G. Zeng, C. Lai, R. Xiao, S. Liu, D. Huang, L. Qin, X. Liu, B. Li, H. Yi, Y. Fu, L. Li, M. Zhang and Z. Wang, Insight into the mechanism of persulfate activated by bone char: Unraveling the role of functional structure of biochar, *Chem. Eng. J.*, 2020, **401**, 126127.

16 S. Liu, C. Lai, B. Li, C. Zhang, M. Zhang, D. Huang, L. Qin, H. Yi, X. Liu, F. Huang, X. Zhou and L. Chen, Role of radical and non-radical pathway in activating persulfate for degradation of p-nitrophenol by sulfur-doped ordered mesoporous carbon, *Chem. Eng. J.*, 2020, **384**, 123304.

17 K. R. Reddy, C. V. Reddy, M. N. Nadagouda, N. P. Shetti, S. Jaesool and T. M. Aminabhavi, Polymeric graphitic carbon

nitride (g-C 3 N 4)-based semiconducting nanostructured materials: Synthesis methods, properties and photocatalytic applications, *J. Environ. Manage.*, 2019, **238**, 25–40.

18 X. Liu, D. Huang, C. Lai, L. Qin, G. Zeng, P. Xu, B. Li, H. Yi and M. Zhang, Peroxidase-Like Activity of Smart Nanomaterials and Their Advanced Application in Colorimetric Glucose Biosensors, *Small*, 2019, **15**, 1900133.

19 C. Zhou, C. Lai, P. Xu, G. Zeng, D. Huang, Z. Li, C. Zhang, M. Cheng, L. Hu, J. Wan, F. Chen, W. Xiong and R. Deng, Rational Design of Carbon-Doped Carbon Nitride/Bi12O17Cl2 Composites: A Promising Candidate Photocatalyst for Boosting Visible-Light-Driven Photocatalytic Degradation of Tetracycline, *ACS Sustainable Chem. Eng.*, 2018, **6**, 6941–6949.

20 Y. Yang, Z. T. Zeng, G. M. Zeng, D. L. Huang, R. Xiao, C. Zhang, C. Y. Zhou, W. P. Xiong, W. J. Wang, M. Cheng, W. J. Xue, H. Guo, X. Tang and D. H. He, Ti3C2 Mxene/porous g-C3N4 interfacial Schottky junction for boosting spatial charge separation in photocatalytic H2O2 production, *Appl. Catal., B*, 2019, **258**, 11.

21 W. Xing, G. Chen, C. Li, Z. Han, Y. Hu and Q. Meng, Doping effect of non-metal group in porous ultrathin g-C3N4 nanosheets towards synergistically improved photocatalytic hydrogen evolution, *Nanoscale*, 2018, **10**, 5239–5245.

22 J. Cai, J. Huang, S. Wang, J. Iocozzia, Z. Sun, J. Sun, Y. Yang, Y. Lai and Z. Lin, Crafting Mussel-Inspired Metal Nanoparticle-Decorated Ultrathin Graphitic Carbon Nitride for the Degradation of Chemical Pollutants and Production of Chemical Resources, *Adv. Mater.*, 2019, **31**, 1806314.

23 C. Zhou, Z. Zeng, G. Zeng, D. Huang, R. Xiao, M. Cheng, C. Zhang, W. Xiong, C. Lai, Y. Yang, W. Wang, H. Yi and B. Li, Visible-light-driven photocatalytic degradation of sulfamethazine by surface engineering of carbon nitride: Properties, degradation pathway and mechanisms, *J. Hazard. Mater.*, 2019, **380**, 120815–120815.

24 J. Xu, Y. Wang and Y. Zhu, Nanoporous Graphitic Carbon Nitride with Enhanced Photocatalytic Performance, *Langmuir*, 2013, **29**, 10566–10572.

25 Y. Gu, M. Ye, Y. Wang, H. Li, H. Zhang, G. Wang, Y. Zhang and H. Zhao, Lignosulfonate functionalized g-C3N4/carbonized wood sponge for highly efficient heavy metal ion scavenging, *J. Mater. Chem. A*, 2020, **8**, 12687–12698.

26 L.-S. Lin, Z.-X. Cong, J. Li, K.-M. Ke, S.-S. Guo, H.-H. Yang and G.-N. Chen, Graphitic-phase C3N4 nanosheets as efficient photosensitizers and pH-responsive drug nanocarriers for cancer imaging and therapy, *J. Mater. Chem. B*, 2014, **2**, 1031–1037.

27 J. Huang, W. Ho and X. Wang, Metal-free disinfection effects induced by graphitic carbon nitride polymers under visible light illumination, *Chem. Commun.*, 2014, **50**, 4338–4340.

28 Y. Li, C. Zhang, D. Shuai, S. Naraginti, D. Wang and W. Zhang, Visible-light-driven photocatalytic inactivation of MS2 by metal-free g-C3N4: Virucidal performance and mechanism, *Water Res.*, 2016, **106**, 249–258.

29 S. Sun and S. Liang, Recent advances in functional mesoporous graphitic carbon nitride (mpg-C3N4) polymers, *Nanoscale*, 2017, **9**, 10544–10578.

30 D. Tang, Y. Chen, M. Yin, Q. Yang, Y. Zhou and L. Zhou, Supramolecular self-assembly production of porous carbon nitride nanosheets with excellent photocatalytic activity by a melamine derivative as doping molecule, *Mater. Sci. Semicond. Process.*, 2020, **105**, 104735.

31 Y. Yang, G. M. Zeng, D. L. Huang, C. Zhang, D. H. He, C. Y. Zhou, W. J. Wang, W. P. Xiong, X. P. Li, B. S. Li, W. Y. Dong and Y. Zhou, Molecular engineering of polymeric carbon nitride for highly efficient photocatalytic oxytetracycline degradation and H2O2 production, *Appl. Catal., B*, 2020, **272**, 14.

32 M. W. Kadi, R. M. Mohamed, A. A. Ismail and D. W. Bahnemann, Soft and hard templates assisted synthesis mesoporous CuO/g-C3N4 heterostructures for highly enhanced and accelerated Hg(II) photoreduction under visible light, *J. Colloid Interface Sci.*, 2020, **580**, 223–233.

33 V. K. Tomer, R. Malik, V. Chaudhary, Y. K. Mishra, L. Kienle, R. Ahuja and L. Lin, Superior visible light photocatalysis and low-operating temperature VOCs sensor using cubic Ag(0)-MoS2 loaded g-CN 3D porous hybrid, *Appl. Mater. Today*, 2019, **16**, 193–203.

34 C. Zhang, Y. Liu, X. Li, H. Chen, T. Wen, Z. Jiang, Y. Ai, Y. Sun, T. Hayat and X. Wang, Highly uranium elimination by crab shells-derived porous graphitic carbon nitride: Batch, EXAFS and theoretical calculations, *Chem. Eng. J.*, 2018, **346**, 406–415.

35 H. Ashrafi, M. Akhond and G. Absalan, Adsorption and photocatalytic degradation of aqueous methylene blue using nanoporous carbon nitride, *J. Photochem. Photobiol., A*, 2020, **396**, 112533.

36 F. Guo, M. Li, H. Ren, X. Huang, K. Shu, W. Shi and C. Lu, Facile bottom-up preparation of Cl-doped porous g-C3N4 nanosheets for enhanced photocatalytic degradation of tetracycline under visible light, *Sep. Purif. Technol.*, 2019, **228**, 115770.

37 Y. Yang, H. Zhao, H. Yang, P. Qiu, B. Zhou and N. Zhang, In situ fabrication of reduced graphene oxide/mesoporous g-C3N4 nanosheets with excellent visible light activity, *J. Environ. Chem. Eng.*, 2018, **6**, 890–897.

38 H.-J. Li, B.-W. Sun, L. Sui, D.-J. Qian and M. Chen, Preparation of water-dispersible porous g-C3N4 with improved photocatalytic activity by chemical oxidation, *Phys. Chem. Chem. Phys.*, 2015, **17**, 3309–3315.

39 X. She, L. Liu, H. Ji, Z. Mo, Y. Li, L. Huang, D. Du, H. Xu and H. Li, Template-free synthesis of 2D porous ultrathin nonmetal-doped g-C3N4 nanosheets with highly efficient photocatalytic H2 evolution from water under visible light, *Appl. Catal., B*, 2016, **187**, 144–153.

40 J. Wang, B. Gao, M. Dou, X. Huang and Z. Ma, A porous g-C3N4 nanosheets containing nitrogen defects for enhanced photocatalytic removal meropenem: Mechanism, degradation pathway and DFT calculation, *Environ. Res.*, 2020, **184**, 109339.

41 S. Zhang, Y. Liu, P. Gu, R. Ma, T. Wen, G. Zhao, L. Li, Y. Ai, C. Hu and X. Wang, Enhanced photodegradation of toxic organic pollutants using dual-oxygen-doped porous g-C3N4: Mechanism exploration from both experimental and DFT studies, *Appl. Catal., B*, 2019, **248**, 1–10.

42 J. Wen, J. Xie, X. Chen and X. Li, A review on g-C3N4-based photocatalysts, *Appl. Surf. Sci.*, 2017, **391**, 72–123.

43 Y. Yang, J. Chen, Z. Mao, N. An, D. Wang and B. D. Fahlman, Ultrathin g-C3N4 nanosheets with an extended visible-light-responsive range for significant enhancement of photocatalysis, *RSC Adv.*, 2017, **7**, 2333–2341.

44 S. Zhang, H. Gao, Y. Huang, X. Wang, T. Hayat, J. Li, X. Xu and X. Wang, Ultrathin g-C3N4 nanosheets coupled with amorphous Cu-doped FeOOH nanoclusters as 2D/0D heterogeneous catalysts for water remediation, *Environ. Sci.: Nano*, 2018, **5**, 1179–1190.

45 L. Wang, Y. Hong, E. Liu, X. Duan, X. Lin and J. Shi, A bottom-up acidification strategy engineered ultrathin g-C3N4 nanosheets towards boosting photocatalytic hydrogen evolution, *Carbon*, 2020, **163**, 234–243.

46 J. Wan, C. Pu, R. Wang, E. Liu, X. Du, X. Bai, J. Fan and X. Hu, A facile dissolution strategy facilitated by H2SO4 to fabricate a 2D metal-free g-C3N4/rGO heterojunction for efficient photocatalytic H2 production, *Int. J. Hydrogen Energy*, 2018, **43**, 7007–7019.

47 P. Li, L. Liu, W. An, H. Wang, H. Guo, Y. Liang and W. Cui, Ultrathin porous g-C3N4 nanosheets modified with AuCu alloy nanoparticles and C-C coupling photothermal catalytic reduction of CO2 to ethanol, *Appl. Catal., B*, 2020, **266**, 118618.

48 J. Li, B. Shen, Z. Hong, B. Lin, B. Gao and Y. Chen, A facile approach to synthesize novel oxygen-doped g-C3N4 with superior visible-light photoreactivity, *Chem. Commun.*, 2012, **48**, 12017–12019.

49 X. Chen, R. Shi, Q. Chen, Z. Zhang, W. Jiang, Y. Zhu and T. Zhang, Three-dimensional porous g-C3N4 for highly efficient photocatalytic overall water splitting, *Nano Energy*, 2019, **59**, 644–650.

50 L. Zhou, J. Feng, B. Qiu, Y. Zhou, J. Lei, M. Xing, L. Wang, Y. Zhou, Y. Liu and J. Zhang, Ultrathin g-C3N4 nanosheet with hierarchical pores and desirable energy band for highly efficient H2O2 production, *Appl. Catal., B*, 2020, **267**, 118396.

51 M. Shalom, M. Guttentag, C. Fettkenhauer, S. Inal, D. Neher, A. Llobet and M. Antonietti, In Situ Formation of Heterojunctions in Modified Graphitic Carbon Nitride: Synthesis and Noble Metal Free Photocatalysis, *Chem. Mater.*, 2014, **26**, 5812–5818.

52 Q. Liu, X. Wang, Q. Yang, Z. Zhang and X. Fang, Mesoporous g-C3N4 nanosheets prepared by calcining a novel supramolecular precursor for high-efficiency photocatalytic hydrogen evolution, *Appl. Surf. Sci.*, 2018, **450**, 46–56.

53 D. Ruan, S. Kim, M. Fujitsuka and T. Majima, Defects rich g-C3N4 with mesoporous structure for efficient photocatalytic H2 production under visible light irradiation, *Appl. Catal., B*, 2018, **238**, 638–646.

54 Y. Jiang, Z. Sun, C. Tang, Y. Zhou, L. Zeng and L. Huang, Enhancement of photocatalytic hydrogen evolution activity of porous oxygen doped g-C3N4 with nitrogen defects induced by changing electron transition, *Appl. Catal., B*, 2019, **240**, 30–38.

55 P. Niu, M. Qiao, Y. Li, L. Huang and T. Zhai, Distinctive defects engineering in graphitic carbon nitride for greatly extended visible light photocatalytic hydrogen evolution, *Nano Energy*, 2018, **44**, 73–81.

56 Q. Liang, Z. Li, Z.-H. Huang, F. Kang and Q.-H. Yang, Holey Graphitic Carbon Nitride Nanosheets with Carbon Vacancies for Highly Improved Photocatalytic Hydrogen Production, *Adv. Funct. Mater.*, 2015, **25**, 6885–6892.

57 L. Jing, D. Wang, Y. Xu, M. Xie, J. Yan, M. He, Z. Song, H. Xu and H. Li, Porous defective carbon nitride obtained by a universal method for photocatalytic hydrogen production from water splitting, *J. Colloid Interface Sci.*, 2020, **566**, 171–182.

58 L. Jiang, X. Yuan, Y. Pan, J. Liang, G. Zeng, Z. Wu and H. Wang, Doping of graphitic carbon nitride for photocatalysis: A review, *Appl. Catal., B*, 2017, **217**, 388–406.

59 L. Zhou, H. Zhang, H. Sun, S. Liu, M. O. Tade, S. Wang and W. Jin, Recent advances in non-metal modification of graphitic carbon nitride for photocatalysis: a historic review, *Catal. Sci. Technol.*, 2016, **6**, 7002–7023.

60 G. Liao, Y. Gong, L. Zhang, H. Gao, G.-J. Yang and B. Fang, Semiconductor polymeric graphitic carbon nitride photocatalysts: the "holy grail" for the photocatalytic hydrogen evolution reaction under visible light, *Energy Environ. Sci.*, 2019, **12**, 2080–2147.

61 X. Liu, R. Ma, L. Zhuang, B. Hu, J. Chen, X. Liu and X. Wang, Recent developments of doped g-C3N4 photocatalysts for the degradation of organic pollutants, *Crit. Rev. Environ. Sci. Technol.*, 2020, 1–40, DOI: 10.1080/10643389.2020.1734433.

62 X. Guo, L. Rao, P. Wang, L. Zhang and Y. Wang, Synthesis of Porous Boron-Doped Carbon Nitride: Adsorption Capacity and Photo-Regeneration Properties, *Int. J. Environ. Res. Public Health*, 2019, **16**, 581.

63 G. Dong, K. Zhao and L. Zhang, Carbon self-doping induced high electronic conductivity and photoreactivity of g-C3N4, *Chem. Commun.*, 2012, **48**, 6178–6180.

64 N. Bao, X. Hu, Q. Zhang, X. Miao, X. Jie and S. Zhou, Synthesis of porous carbon-doped g-C3N4 nanosheets with enhanced visible-light photocatalytic activity, *Appl. Surf. Sci.*, 2017, **403**, 682–690.

65 X. Ma, Y. Lv, J. Xu, Y. Liu, R. Zhang and Y. Zhu, A Strategy of Enhancing the Photoactivity of g-C3N4 via Doping of Nonmetal Elements: A First-Principles Study, *J. Phys. Chem. C*, 2012, **116**, 23485–23493.

66 S. Cao, B. Fan, Y. Feng, H. Chen, F. Jiang and X. Wang, Sulfur-doped g-C3N4 nanosheets with carbon vacancies: General synthesis and improved activity for simulated solar-light photocatalytic nitrogen fixation, *Chem. Eng. J.*, 2018, **353**, 147–156.

67 H. Yu, L. Shang, T. Bian, R. Shi, G. I. N. Waterhouse, Y. Zhao, C. Zhou, L.-Z. Wu, C.-H. Tung and T. Zhang, Nitrogen-Doped

Porous Carbon Nanosheets Templated from g-C3N4 as Metal-Free Electrocatalysts for Efficient Oxygen Reduction Reaction, *Adv. Mater.*, 2016, **28**, 5080–5086.
68 C. Hu, M.-S. Wang, C.-H. Chen, Y.-R. Chen, P.-H. Huang and K.-L. Tung, Phosphorus-doped g-C3N4 integrated photocatalytic membrane reactor for wastewater treatment, *J. Membr. Sci.*, 2019, **580**, 1–11.
69 S. Zhao, Y. Zhang, Y. Wang, Y. Zhou, K. Qiu, C. Zhang, J. Fang and X. Sheng, Ionic liquid-assisted synthesis of Br-modified g-C3N4 semiconductors with high surface area and highly porous structure for photoredox water splitting, *J. Power Sources*, 2017, **370**, 106–113.
70 Z.-A. Lan, G. Zhang and X. Wang, A facile synthesis of Br-modified g-C3N4 semiconductors for photoredox water splitting, *Appl. Catal., B*, 2016, **192**, 116–125.
71 Y. Yang, H. Jin, C. Zhang, H. Gan, F. Yi and H. Wang, Nitrogen-deficient modified P–Cl co-doped graphitic carbon nitride with enhanced photocatalytic performance, *J. Alloys Compd.*, 2020, **821**, 153439.
72 Y. Gao, F. Hou, S. Hu, B. Wu and B. Jiang, Synchronization iodine surface modification and lattice doping porous carbon nitride for photocatalytic hydrogen production, *Appl. Surf. Sci.*, 2019, **481**, 1089–1095.
73 J. Barrio, A. Grafmüller, J. Tzadikov and M. Shalom, Halogen-hydrogen bonds: A general synthetic approach for highly photoactive carbon nitride with tunable properties, *Appl. Catal., B*, 2018, **237**, 681–688.
74 J. Jiang, S. Cao, C. Hu and C. Chen, A comparison study of alkali metal-doped g-C3N4 for visible-light photocatalytic hydrogen evolution, *Chin. J. Catal.*, 2017, **38**, 1981–1989.
75 W. Miao, Y. Liu, X. Chen, Y. Zhao and S. Mao, Tuning layered Fe-doped g-C3N4 structure through pyrolysis for enhanced Fenton and photo-Fenton activities, *Carbon*, 2020, **159**, 461–470.
76 W. Wu, Z. Ruan, J. Li, Y. Li, Y. Jiang, X. Xu, D. Li, Y. Yuan and K. Lin, In Situ Preparation and Analysis of Bimetal Co-doped Mesoporous Graphitic Carbon Nitride with Enhanced Photocatalytic Activity, *Nano-Micro Lett.*, 2019, **11**, 10.
77 J.-C. Wang, C.-X. Cui, Y. Li, L. Liu, Y.-P. Zhang and W. Shi, Porous Mn doped g-C3N4 photocatalysts for enhanced synergetic degradation under visible-light illumination, *J. Hazard. Mater.*, 2017, **339**, 43–53.
78 J. Lin, W. Tian, H. Zhang, X. Duan, H. Sun and S. Wang, Graphitic Carbon Nitride-Based Z-Scheme Structure for Photocatalytic CO2 Reduction, *Energy Fuels*, 2021, **35**, 7–24.
79 J. Low, J. Yu, M. Jaroniec, S. Wageh and A. A. Al-Ghamdi, Heterojunction Photocatalysts, *Adv. Mater.*, 2017, **29**, 1601694.
80 S. Wu, H.-J. Zhao, C.-F. Li, J. Liu, W. Dong, H. Zhao, C. Wang, Y. Liu, Z.-Y. Hu, L. Chen, Y. Li and B.-L. Su, Type II heterojunction in hierarchically porous zinc oxide/graphitic carbon nitride microspheres promoting photocatalytic activity, *J. Colloid Interface Sci.*, 2019, **538**, 99–107.
81 Z. Dong, J. Pan, B. Wang, Z. Jiang, C. Zhao, J. Wang, C. Song, Y. Zheng, C. Cui and C. Li, The p-n-type Bi5O7I-modified porous C3N4 nano-heterojunction for enhanced visible light photocatalysis, *J. Alloys Compd.*, 2018, **747**, 788–795.
82 J. Lv, K. Dai, J. Zhang, Q. Liu, C. Liang and G. Zhu, Facile constructing novel 2D porous g-C3N4/BiOBr hybrid with enhanced visible-light-driven photocatalytic activity, *Sep. Purif. Technol.*, 2017, **178**, 6–17.
83 A. Meng, L. Zhang, B. Cheng and J. Yu, Dual Cocatalysts in TiO2 Photocatalysis, *Adv. Mater.*, 2019, **31**, 1807660.
84 H. Zhang, W. Tian, X. Duan, H. Sun, Y. Shen, G. Shao and S. Wang, Functional carbon nitride materials for water oxidation: from heteroatom doping to interface engineering, *Nanoscale*, 2020, **12**, 6937–6952.
85 H. Zhang, W. Tian, L. Zhou, H. Sun, M. Tade and S. Wang, Monodisperse Co3O4 quantum dots on porous carbon nitride nanosheets for enhanced visible-light-driven water oxidation, *Appl. Catal., B*, 2018, **223**, 2–9.
86 W. Chen, M. Liu, S. Wei, X. Li, L. Mao and W. Shangguan, Solid-state synthesis of ultrathin MoS2 as a cocatalyst on mesoporous g-C3N4 for excellent enhancement of visible light photoactivity, *J. Alloys Compd.*, 2020, **836**, 155401.
87 J. Xu, X. Zheng, Z. Feng, Z. Lu, Z. Zhang, W. Huang, Y. Li, D. Vuckovic, Y. Li, S. Dai, G. Chen, K. Wang, H. Wang, J. K. Chen, W. Mitch and Y. Cui, Organic wastewater treatment by a single-atom catalyst and electrolytically produced H2O2, *Nat. Sustain.*, 2021, **4**, 233–241.
88 Y. Chen, S. Ji, C. Chen, Q. Peng, D. Wang and Y. Li, Single-Atom Catalysts: Synthetic Strategies and Electrochemical Applications, *Joule*, 2018, **2**, 1242–1264.
89 H. Zhang, W. Tian, X. Duan, H. Sun, S. Liu and S. Wang, Catalysis of a Single Transition Metal Site for Water Oxidation: From Mononuclear Molecules to Single Atoms, *Adv. Mater.*, 2020, **32**, 1904037.
90 S. Wang, J. Li, Q. Li, X. Bai and J. Wang, Metal single-atom coordinated graphitic carbon nitride as an efficient catalyst for CO oxidation, *Nanoscale*, 2020, **12**, 364–371.
91 X. Li, S. Zhao, X. Duan, H. Zhang, S.-Z. Yang, P. Zhang, S. P. Jiang, S. Liu, H. Sun and S. Wang, Coupling hydrothermal and photothermal single-atom catalysis toward excellent water splitting to hydrogen, *Appl. Catal., B*, 2021, **283**, 119660.
92 Y. Yang, G. Zeng, D. Huang, C. Zhang, D. He, C. Zhou, W. Wang, W. Xiong, B. Song, H. Yi, S. Ye and X. Ren, In Situ Grown Single-Atom Cobalt on Polymeric Carbon Nitride with Bidentate Ligand for Efficient Photocatalytic Degradation of Refractory Antibiotics, *Small*, 2020, **16**, 2001634.
93 W. Zhao, J. Wang, R. Yin, B. Li, X. Huang, L. Zhao and L. Qian, Single-atom Pt supported on holey ultrathin g-C3N4 nanosheets as efficient catalyst for Li-O2 batteries, *J. Colloid Interface Sci.*, 2020, **564**, 28–36.
94 S. Ye, M. Yan, X. Tan, J. Liang, G. Zeng, H. Wu, B. Song, C. Zhou, Y. Yang and H. Wang, Facile assembled biochar-based nanocomposite with improved graphitization for efficient photocatalytic activity driven by visible light, *Appl. Catal., B*, 2019, **250**, 78–88.

95 Y. Sheng, Z. Wei, H. Miao, W. Yao, H. Li and Y. Zhu, Enhanced organic pollutant photodegradation via adsorption/photocatalysis synergy using a 3D g-C3N4/TiO2 free-separation photocatalyst, *Chem. Eng. J.*, 2019, **370**, 287–294.

96 M. Ramalingam, V. K. Ponnusamy and S. N. Sangilimuthu, A nanocomposite consisting of porous graphitic carbon nitride nanosheets and oxidized multiwalled carbon nanotubes for simultaneous stripping voltammetric determination of cadmium(II), mercury(II), lead(II) and zinc(II), *Microchim. Acta*, 2019, **186**, 69.

97 Y. Wu, H. Pang, Y. Liu, X. Wang, S. Yu, D. Fu, J. Chen and X. Wang, Environmental remediation of heavy metal ions by novel-nanomaterials: A review, *Environ. Pollut.*, 2019, **246**, 608–620.

98 B. Ou, J. Wang, Y. Wu, S. Zhao and Z. Wang, Efficient removal of Cr (VI) by magnetic and recyclable calcined CoFe-LDH/g-C3N4 via the synergy of adsorption and photocatalysis under visible light, *Chem. Eng. J.*, 2020, **380**, 122600.

99 M. Li, B. Wang, M. Yang, Q. Li, D. G. Calatayud, S. Zhang, H. Wang, L. Wang and B. Mao, Promoting mercury removal from desulfurization slurry via S-doped carbon nitride/graphene oxide 3D hierarchical framework, *Sep. Purif. Technol.*, 2020, **239**, 116515.

100 X. Zhao, D. Pan, X. Chen, R. Li, T. Jiang, W. Wang, G. Li and D. Y. C. Leung, g-C3N4 photoanode for photoelectrocatalytic synergistic pollutant degradation and hydrogen evolution, *Appl. Surf. Sci.*, 2019, **467–468**, 658–665.

101 J. Safaei, H. Ullah, N. A. Mohamed, M. F. Mohamad Noh, M. F. Soh, A. A. Tahir, N. Ahmad Ludin, M. A. Ibrahim, W. N. R. Wan Isahak and M. A. Mat Teridi, Enhanced photoelectrochemical performance of Z-scheme g-C3N4/BiVO4 photocatalyst, *Appl. Catal., B*, 2018, **234**, 296–310.

102 Q. Song, J. Li, L. Wang, Y. Qin, L. Pang and H. Liu, Stable single-atom cobalt as a strong coupling bridge to promote electron transfer and separation in photoelectrocatalysis, *J. Catal.*, 2019, **370**, 176–185.

103 J. Hu, C. Chen, T. Hu, J. Li, H. Lu, Y. Zheng, X. Yang, C. Guo and C. M. Li, Metal-free heterojunction of black phosphorus/oxygen-enriched porous g-C3N4 as an efficient photocatalyst for Fenton-like cascade water purification, *J. Mater. Chem. A*, 2020, **8**, 19484–19492.

104 J. Jiang, X. Wang, Y. Liu, Y. Ma, T. Li, Y. Lin, T. Xie and S. Dong, Photo-Fenton degradation of emerging pollutants over Fe-POM nanoparticle/porous and ultrathin g-C3N4 nanosheet with rich nitrogen defect: Degradation mechanism, pathways, and products toxicity assessment, *Appl. Catal., B*, 2020, **278**, 119349.

105 C. Liu, L. Liu, X. Tian, Y. Wang, R. Li, Y. Zhang, Z. Song, B. Xu, W. Chu, F. Qi and A. Ikhlaq, Coupling metal–organic frameworks and g-C3N4 to derive Fe@N-doped graphene-like carbon for peroxymonosulfate activation: Upgrading framework stability and performance, *Appl. Catal., B*, 2019, **255**, 117763.

106 W. Feng, J. Fang, G. Zhou, L. Zhang, S. Lu, S. Wu, Y. Chen, Y. Ling and Z. Fang, Rationally designed Bi@BiOCl/g-C3N4 heterostructure with exceptional solar-driven photocatalytic activity, *Mol. Catal.*, 2017, **434**, 69–79.

107 X. Du, X. Yi, P. Wang, J. Deng and C.-C. Wang, Enhanced photocatalytic Cr(VI) reduction and diclofenac sodium degradation under simulated sunlight irradiation over MIL-100(Fe)/g-C3N4 heterojunctions, *Chin. J. Catal.*, 2019, **40**, 70–79.

108 H. Wang, Q. Li, S. Zhang, Z. Chen, W. Wang, G. Zhao, L. Zhuang, B. Hu and X. Wang, Visible-light-driven N2-g-C3N4 as a highly stable and efficient photocatalyst for bisphenol A and Cr(VI) removal in binary systems, *Catal. Today*, 2019, **335**, 110–116.

109 L. Qin, Z. Zeng, G. Zeng, C. Lai, A. Duan, R. Xiao, D. Huang, Y. Fu, H. Yi, B. Li, X. Liu, S. Liu, M. Zhang and D. Jiang, Cooperative catalytic performance of bimetallic Ni-Au nanocatalyst for highly efficient hydrogenation of nitroaromatics and corresponding mechanism insight, *Appl. Catal., B*, 2019, **259**, 118035.

110 L. Qin, D. Huang, P. Xu, G. Zeng, C. Lai, Y. Fu, H. Yi, B. Li, C. Zhang, M. Cheng, C. Zhou and X. Wen, In-situ deposition of gold nanoparticles onto polydopamine-decorated g-C3N4 for highly efficient reduction of nitroaromatics in environmental water purification, *J. Colloid Interface Sci.*, 2019, **534**, 357–369.

111 Z. Hu, J. Zhou, Y. Ai, L. Liu, L. Qi, R. Jiang, H. Bao, J. Wang, J. Hu, H.-B. Sun and Q. Liang, Two dimensional Rh/Fe3O4/g-C3N4-N enabled hydrazine mediated catalytic transfer hydrogenation of nitroaromatics: A predictable catalyst model with adjoining Rh, *J. Catal.*, 2018, **368**, 20–30.

112 V. Balakumar, H. Kim, J. W. Ryu, R. Manivannan and Y.-A. Son, Uniform assembly of gold nanoparticles on S-doped g-C3N4 nanocomposite for effective conversion of 4-nitrophenol by catalytic reduction, *J. Mater. Sci. Technol.*, 2020, **40**, 176–184.

113 Y. Fu, L. Qin, D. Huang, G. Zeng, C. Lai, B. Li, J. He, H. Yi, M. Zhang, M. Cheng and X. Wen, Chitosan functionalized activated coke for Au nanoparticles anchoring: Green synthesis and catalytic activities in hydrogenation of nitrophenols and azo dyes, *Appl. Catal., B*, 2019, **255**, 117740.

114 J. Zhang and Z. Ma, Porous g-C3N4 with enhanced adsorption and visible-light photocatalytic performance for removing aqueous dyes and tetracycline hydrochloride, *Chin. J. Chem. Eng.*, 2018, **26**, 753–760.

115 J.-Y. Zhang, S.-H. Zhang, J. Li, X.-C. Zheng and X.-X. Guan, Constructing of 3D graphene aerogel-g-C3N4 metal-free heterojunctions with superior purification efficiency for organic dyes, *J. Mol. Liq.*, 2020, **310**, 113242.

116 D. P. Dutta and D. Dagar, Efficient Selective Sorption of Cationic Organic Pollutant from Water and Its Photocatalytic Degradation by AlVO4/g-C3N4 Nanocomposite, *J. Nanosci. Nanotechnol.*, 2020, **20**, 2179–2194.

117 J. Di, J. Xia, X. Li, M. Ji, H. Xu, Z. Chen and H. Li, Constructing confined surface carbon defects in ultrathin graphitic carbon nitride for photocatalytic free radical manipulation, *Carbon*, 2016, **107**, 1–10.

118 H. Shen, M. Li, W. Guo, G. Li and C. Xu, P, K co-doped porous g-C3N4 with enhanced photocatalytic activity synthesized in vapor and self-producing NH3 atmosphere, *Appl. Surf. Sci.*, 2020, **507**, 145086.
119 Z. Wang, H. Wang, Z. Zeng, G. Zeng, P. Xu, R. Xiao, D. Huang, X. Chen, L. He, C. Zhou, Y. Yang, Z. Wang, W. Wang and W. Xiong, Metal-organic frameworks derived Bi2O2CO3/porous carbon nitride: A nanosized Z-scheme systems with enhanced photocatalytic activity, *Appl. Catal., B*, 2020, **267**, 118700.
120 F. Wang, P. Chen, Y. Feng, Z. Xie, Y. Liu, Y. Su, Q. Zhang, Y. Wang, K. Yao, W. Lv and G. Liu, Facile synthesis of N-doped carbon dots/g-C3N4 photocatalyst with enhanced visible-light photocatalytic activity for the degradation of indomethacin, *Appl. Catal., B*, 2017, **207**, 103–113.
121 S. Li, W. Shi, W. Liu, H. Li, W. Zhang, J. Hu, Y. Ke, W. Sun and J. Ni, A duodecennial national synthesis of antibiotics in China's major rivers and seas (2005–2016), *Sci. Total Environ.*, 2018, **615**, 906–917.
122 L. Lonappan, S. K. Brar, R. K. Das, M. Verma and R. Y. Surampalli, Diclofenac and its transformation products: Environmental occurrence and toxicity - A review, *Environ. Int.*, 2016, **96**, 127–138.
123 S. Luo, L. Gao, Z. Wei, R. Spinney, D. D. Dionysiou, W.-P. Hu, L. Chai and R. Xiao, Kinetic and mechanistic aspects of hydroxyl radical–mediated degradation of naproxen and reaction intermediates, *Water Res.*, 2018, **137**, 233–241.
124 L. Sbardella, I. Velo-Gala, J. Comas, I. Rodríguez-Roda Layret, A. Fenu and W. Gernjak, The impact of wastewater matrix on the degradation of pharmaceutically active compounds by oxidation processes including ultraviolet radiation and sulfate radicals, *J. Hazard. Mater.*, 2019, **380**, 120869.
125 J. Jiang, X. Wang, C. Zhang, T. Li, Y. Lin, T. Xie and S. Dong, Porous 0D/3D NiCo2O4/g-C3N4 accelerate emerging pollutant degradation in PMS/vis system: Degradation mechanism, pathway and toxicity assessment, *Chem. Eng. J.*, 2020, **397**, 125356.
126 L. Zhang, F. Sun, D. Wu, W. Yan and Y. Zhou, Biological conversion of sulfamethoxazole in an autotrophic denitrification system, *Water Res.*, 2020, **185**, 116156.
127 G. Liu, Z. Zhang, M. Lv, H. Wang, D. Chen and Y. Feng, Photodegradation performance and transformation mechanisms of sulfamethoxazole by porous g-C3N4 modified with ammonia bicarbonate, *Sep. Purif. Technol.*, 2020, **235**, 116172.
128 X. Zheng, Q. Zhang, T. Chen, Y. Wu, J. Hao, C. Tan, P. Chen, F. Wang, H. Liu, W. Lv and G. Liu, A novel synthetic carbon and oxygen doped stalactite-like g-C3N4 for broad-spectrum-driven indometacin degradation, *J. Hazard. Mater.*, 2020, **386**, 121961.
129 X. Huo, Y. Yang, Q. Niu, Y. Zhu, G. Zeng, C. Lai, H. Yi, M. Li, Z. An, D. Huang, Y. Fu, B. Li, L. Li and M. Zhang, A direct Z-scheme oxygen vacant BWO/oxygen-enriched graphitic carbon nitride polymer heterojunction with enhanced photocatalytic activity, *Chem. Eng. J.*, 2021, **403**, 126363.
130 W. Wang, Q. Niu, G. Zeng, C. Zhang, D. Huang, B. Shao, C. Zhou, Y. Yang, Y. Liu, H. Guo, W. Xiong, L. Lei, S. Liu, H. Yi, S. Chen and X. Tang, 1D porous tubular g-C3N4 capture black phosphorus quantum dots as 1D/0D metal-free photocatalysts for oxytetracycline hydrochloride degradation and hexavalent chromium reduction, *Appl. Catal., B*, 2020, **273**, 119051.
131 S. Ye, G. Zeng, X. Tan, H. Wu, J. Liang, B. Song, N. Tang, P. Zhang, Y. Yang, Q. Chen and X. Li, Nitrogen-doped biochar fiber with graphitization from Boehmeria nivea for promoted peroxymonosulfate activation and non-radical degradation pathways with enhancing electron transfer, *Appl. Catal., B*, 2020, **269**, 118850.
132 C.-H. Han, H.-D. Park, S.-B. Kim, V. Yargeau, J.-W. Choi, S.-H. Lee and J.-A. Park, Oxidation of tetracycline and oxytetracycline for the photo-Fenton process: Their transformation products and toxicity assessment, *Water Res.*, 2020, **172**, 115514.
133 K. Wu, D. Chen, S. Lu, J. Fang, X. Zhu, F. Yang, T. Pan and Z. Fang, Supramolecular self-assembly synthesis of noble-metal-free (C, Ce) co-doped g-C3N4 with porous structure for highly efficient photocatalytic degradation of organic pollutants, *J. Hazard. Mater.*, 2020, **382**, 121027.
134 Y. Yang, C. Zhang, D. Huang, G. Zeng, J. Huang, C. Lai, C. Zhou, W. Wang, H. Guo, W. Xue, R. Deng, M. Cheng and W. Xiong, Boron nitride quantum dots decorated ultrathin porous g-C3N4: Intensified exciton dissociation and charge transfer for promoting visible-light-driven molecular oxygen activation, *Appl. Catal., B*, 2019, **245**, 87–99.
135 L. Zhao, D. Xiao, Y. Liu, H. Xu, H. Nan, D. Li, Y. Kan and X. Cao, Biochar as simultaneous shelter, adsorbent, pH buffer, and substrate of Pseudomonas citronellolis to promote biodegradation of high concentrations of phenol in wastewater, *Water Res.*, 2020, **172**, 115494.
136 Y. Li, Z. Ruan, Y. He, J. Li, K. Li, Y. Jiang, X. Xu, Y. Yuan and K. Lin, In situfabrication of hierarchically porous g-C3N4 and understanding on its enhanced photocatalytic activity based on energy absorption, *Appl. Catal., B*, 2018, **236**, 64–75.
137 N. Liu, N. Lu, H. Yu, S. Chen and X. Quan, Efficient day-night photocatalysis performance of 2D/2D Ti3C2/Porous g-C3N4 nanolayers composite and its application in the degradation of organic pollutants, *Chemosphere*, 2020, **246**, 125760.
138 Y. Gao, Y. Zhu, L. Lyu, Q. Zeng, X. Xing and C. Hu, Electronic Structure Modulation of Graphitic Carbon Nitride by Oxygen Doping for Enhanced Catalytic Degradation of Organic Pollutants through Peroxymonosulfate Activation, *Environ. Sci. Technol.*, 2018, **52**, 14371–14380.
139 S. Xu, Y. Zhao, X. Sun, X. Zheng, S. Ni, Q. Yue and B. Gao, Introduction of porous structure via facile carbon-dot modulation: A feasible and promising approach for improving the photocatalytic capability of sulfur doped g-C3N4, *Catal. Today*, 2019, **335**, 502–510.
140 H. Sun, F. Guo, J. Pan, W. Huang, K. Wang and W. Shi, One-pot thermal polymerization route to prepare

N-deficient modified g-C3N4 for the degradation of tetracycline by the synergistic effect of photocatalysis and persulfate-based advanced oxidation process, *Chem. Eng. J.*, 2021, **406**, 126844.

141 W. Xu, S. Lai, S. C. Pillai, W. Chu, Y. Hu, X. Jiang, M. Fu, X. Wu, F. Li and H. Wang, Visible light photocatalytic degradation of tetracycline with porous Ag/graphite carbon nitride plasmonic composite: Degradation pathways and mechanism, *J. Colloid Interface Sci.*, 2020, **574**, 110–121.

142 L. Jiang, X. Yuan, G. Zeng, J. Liang, Z. Wu, H. Yu, D. Mo, H. Wang, Z. Xiao and C. Zhou, Nitrogen self-doped g-C3N4 nanosheets with tunable band structures for enhanced photocatalytic tetracycline degradation, *J. Colloid Interface Sci.*, 2019, **536**, 17–29.

143 F. C. Moreira, J. Soler, A. Fonseca, I. Saraiva, R. A. R. Boaventura, E. Brillas and V. J. P. Vilar, Incorporation of electrochemical advanced oxidation processes in a multistage treatment system for sanitary landfill leachate, *Water Res.*, 2015, **81**, 375–387.

144 D. Ma, H. Yi, C. Lai, X. Liu, X. Huo, Z. An, L. Li, Y. Fu, B. Li, M. Zhang, L. Qin, S. Liu and L. Yang, Critical review of advanced oxidation processes in organic wastewater treatment, *Chemosphere*, 2021, **275**, 130104.

145 H. Wang, Z. Cheng, H. Yuan, N. Zhu, Z. Lou and P. Otieno, Occurrence of banned and commonly used pesticide residues in concentrated leachate: Implications for ecological risk assessment, *Sci. Total Environ.*, 2020, **710**, 136287.

146 J. N. Göde, D. Hoefling Souza, V. Trevisan and E. Skoronski, Application of the Fenton and Fenton-like processes in the landfill leachate tertiary treatment, *J. Environ. Chem. Eng.*, 2019, **7**, 103352.

147 K. Roy and V. S. Moholkar, Sulfadiazine degradation using hybrid AOP of heterogeneous Fenton/persulfate system coupled with hydrodynamic cavitation, *Chem. Eng. J.*, 2020, **386**, 121294.

148 M. Anjum, R. Kumar and M. A. Barakat, Synthesis of Cr2O3/C3N4 composite for enhancement of visible light photocatalysis and anaerobic digestion of wastewater sludge, *J. Environ. Manage.*, 2018, **212**, 65–76.

149 P. Gautam, S. Kumar and S. Lokhandwala, Advanced oxidation processes for treatment of leachate from hazardous waste landfill: A critical review, *J. Cleaner Prod.*, 2019, **237**, 117639.

150 D. E. Meeroff, F. Bloetscher, D. V. Reddy, F. Gasnier, S. Jain, A. McBarnette and H. Hamaguchi, Application of photochemical technologies for treatment of landfill leachate, *J. Hazard. Mater.*, 2012, **209–210**, 299–307.

151 L. Hu, Y. Liu, G. Zeng, G. Chen, J. Wan, Y. Zeng, L. Wang, H. Wu, P. Xu, C. Zhang, M. Cheng and T. Hu, Organic matters removal from landfill leachate by immobilized Phanerochaete chrysosporium loaded with graphitic carbon nitride under visible light irradiation, *Chemosphere*, 2017, **184**, 1071–1079.

152 H. Zhang, Z. Liu, Y. Li, C. Zhang, Y. Wang, W. Zhang, L. Wang, L. Niu, P. Wang and C. Wang, Intimately coupled TiO2/g-C3N4 photocatalysts and in-situ cultivated biofilms enhanced nitrate reduction in water, *Appl. Surf. Sci.*, 2020, **503**, 144092.

153 Y. Shi, J. Huang, G. Zeng, W. Cheng and J. Hu, Photocatalytic membrane in water purification: is it stepping closer to be driven by visible light?, *J. Membr. Sci.*, 2019, **584**, 364–392.

154 K. G. Zhou, D. McManus, E. Prestat, X. Zhong, Y. Y. Shin, H. L. Zhang, S. J. Haigh and C. Casiraghi, Self-catalytic membrane photo-reactor made of carbon nitride nanosheets, *J. Mater. Chem. A*, 2016, **4**, 11666–11671.

155 Y. Jiang, P. Biswas and J. D. Fortner, A review of recent developments in graphene-enabled membranes for water treatment, *Environ. Sci.: Water Res. Technol.*, 2016, **2**, 915–922.

156 Z. Liu, R. Cao and M. Zhang, Preparation and Property of Polyethersulfone Ultrafiltration Membranes with Mesoporous-graphitic-C_3N_4/Ag, *Wuji Cailiao Xuebao*, 2019, **34**, 478–486.

157 F. Gao, X. Du, X. Hao, X. Ma, L. Chang, N. Han, G. Guan and K. Tang, A novel electrical double-layer ion transport carbon-based membrane with 3D porous structure: High permselectivity for dilute zinc ion separation, *Chem. Eng. J.*, 2020, **380**, 122413.

158 Y. Shi, D. Wan, J. Huang, Y. Liu and J. Li, Stable LBL self-assembly coating porous membrane with 3D heterostructure for enhanced water treatment under visible light irradiation, *Chemosphere*, 2020, **252**, 126581.

159 L. Chen, W. Xiang, H. Wu, S. Ouyang, B. Zhou, Y. Zeng, Y. Chen and Y. Kuzyakov, Tree species identity surpasses richness in affecting soil microbial richness and community composition in subtropical forests, *Soil Biol. Biochem.*, 2019, **130**, 113–121.

160 W. Wang, C. Zhou, Y. Yang, G. Zeng, C. Zhang, Y. Zhou, J. Yang, D. Huang, H. Wang, W. Xiong, X. Li, Y. Fu, Z. Wang, Q. He, M. Jia and H. Luo, Carbon nitride based photocatalysts for solar photocatalytic disinfection, can we go further?, *Chem. Eng. J.*, 2021, **404**, 126540.

161 D. Wang, S. C. Pillai, S. H. Ho, J. Zeng, Y. Li and D. D. Dionysiou, Plasmonic-based nanomaterials for environmental remediation, *Appl. Catal., B*, 2018, **237**, 721–741.

162 D. Wang, B. Zhu, X. He, Z. Zhu, G. Hutchins, P. Xu and W.-N. Wang, Iron oxide nanowire-based filter for inactivation of airborne bacteria, *Environ. Sci.: Nano*, 2018, **5**, 1096–1106.

163 W. Wang, Z. Zeng, G. Zeng, C. Zhang, R. Xiao, C. Zhou, W. Xiong, Y. Yang, L. Lei, Y. Liu, D. Huang, M. Cheng, Y. Yang, Y. Fu, H. Luo and Y. Zhou, Sulfur doped carbon quantum dots loaded hollow tubular g-C3N4 as novel photocatalyst for destruction of Escherichia coli and tetracycline degradation under visible light, *Chem. Eng. J.*, 2019, **378**, 122132.

164 J. Xu, Z. Wang and Y. Zhu, Enhanced Visible-Light-Driven Photocatalytic Disinfection Performance and Organic Pollutant Degradation Activity of Porous g-C3N4 Nanosheets, *ACS Appl. Mater. Interfaces*, 2017, **9**, 27727–27735.

165 Y. Chen, P. Wang, Y. Liang, M. Zhao, Y. Jiang, G. Wang, P. Zou, J. Zeng, Y. Zhang and Y. Wang, Fabrication of a three-dimensional porous Z-scheme silver/silver bromide/graphitic carbon nitride@nitrogen-doped graphene aerogel with enhanced visible-light photocatalytic and antibacterial activities, *J. Colloid Interface Sci.*, 2019, **536**, 389–398.

166 J. H. Thurston, N. M. Hunter, L. J. Wayment and K. A. Cornell, Urea-derived graphitic carbon nitride (u-g-C3N4) films with highly enhanced antimicrobial and sporicidal activity, *J. Colloid Interface Sci.*, 2017, **505**, 910–918.

167 R. Wang, X. Kong, W. Zhang, W. Zhu, L. Huang, J. Wang, X. Zhang, X. Liu, N. Hu, Y. Suo and J. Wang, Mechanism insight into rapid photocatalytic disinfection of Salmonella based on vanadate QDs-interspersed g-C3N4 heterostructures, *Appl. Catal., B*, 2018, **225**, 228–237.

168 S. Kang, W. Huang, L. Zhang, M. He, S. Xu, D. Sun and X. Jiang, Moderate Bacterial Etching Allows Scalable and Clean Delamination of g-C3N4 with Enriched Unpaired Electrons for Highly Improved Photocatalytic Water Disinfection, *ACS Appl. Mater. Interfaces*, 2018, **10**, 13796–13804.

169 O. K. Dalrymple, E. Stefanakos, M. A. Trotz and D. Y. Goswami, A review of the mechanisms and modeling of photocatalytic disinfection, *Appl. Catal., B*, 2010, **98**, 27–38.

170 J. Xu, Q. Gao, X. Bai, Z. Wang and Y. Zhu, Enhanced visible-light-induced photocatalytic degradation and disinfection activities of oxidized porous g-C3N4 by loading Ag nanoparticles, *Catal. Today*, 2019, **332**, 227–235.

171 J. H. Thurston, N. M. Hunter and K. A. Cornell, Preparation and characterization of photoactive antimicrobial graphitic carbon nitride (g-C3N4) films, *RSC Adv.*, 2016, **6**, 42240–42248.

172 C. Zhang, Y. Li, D. Shuai, W. Zhang, L. Niu, L. Wang and H. Zhang, Visible-light-driven, water-surface-floating antimicrobials developed from graphitic carbon nitride and expanded perlite for water disinfection, *Chemosphere*, 2018, **208**, 84–92.

173 J. Song, X. Wang, J. Ma, X. Wang, J. Wang, S. Xia and J. Zhao, Removal of Microcystis aeruginosa and Microcystin-LR using a graphitic-C3N4/TiO2 floating photocatalyst under visible light irradiation, *Chem. Eng. J.*, 2018, **348**, 380–388.

174 D. Wang, Y. Ao and P. Wang, Effective inactivation of Microcystis aeruginosa by a novel Z-scheme composite photocatalyst under visible light irradiation, *Sci. Total Environ.*, 2020, **746**, 141149.

175 J. Song, X. Wang, J. Ma, X. Wang, J. Wang and J. Zhao, Visible-light-driven in situ inactivation of Microcystis aeruginosa with the use of floating g-C3N4 heterojunction photocatalyst: Performance, mechanisms and implications, *Appl. Catal., B*, 2018, **226**, 83–92.

176 Y. Xu, B. Hu, J. Liu, K. Tao, R. Wang, Y. Ren, X. Zhao, J. Xu and X. Song, Visible light-activated degradation of microcystin-LR by ultrathin g-C_3N_4 nanosheets-based heterojunction photocatalyst, *J. Am. Ceram. Soc.*, 2019, **103**, 1281–1292.

177 N. He, S. Cao, L. Zhang, Z. Tian, H. Chen and F. Jiang, Enhanced photocatalytic disinfection of Escherichia coli K-12 by porous g-C3N4 nanosheets: Combined effect of photo-generated and intracellular ROSs, *Chemosphere*, 2019, **235**, 1116–1124.

178 H. Liu, S. Ma, L. Shao, H. Liu, Q. Gao, B. Li, H. Fu, S. Fu, H. Ye, F. Zhao and J. Zhou, Defective engineering in graphitic carbon nitride nanosheet for efficient photocatalytic pathogenic bacteria disinfection, *Appl. Catal., B*, 2020, **261**, 118201.

179 P. Yadav, S. T. Nishanthi, B. Purohit, A. Shanavas and K. Kailasam, Metal-free visible light photocatalytic carbon nitride quantum dots as efficient antibacterial agents: An insight study, *Carbon*, 2019, **152**, 587–597.

180 D. Thakur, Q. T. H. Ta and J. S. Noh, Photon-Induced Superior Antibacterial Activity of Palladium-Decorated, Magnetically Separable Fe3O4/Pd/mpg-C3N4 Nanocomposites, *Molecules*, 2019, **24**, 3888.

181 Y. Xu, B. Hu, J. Liu, K. Tao, R. Wang, Y. Ren, X. Zhao, J. Xu and X. Song, Visible light-activated degradation of microcystin-LR by ultrathin g-C3N4 nanosheets-based heterojunction photocatalyst, *J. Am. Ceram. Soc.*, 2020, **103**, 1281–1292.

182 G. Fan, B. Du, J. Zhou, W. Yu, Z. Chen and S. Yang, Stable Ag2O/g-C3N4 p-n heterojunction photocatalysts for efficient inactivation of harmful algae under visible light, *Appl. Catal., B*, 2020, **265**, 118610.

